

**TASI 2008 lectures on Collider Signals II:
missing E_T signatures and dark matter connection**

Howard Baer*

*Homer L. Dodge Department of Physics and Astronomy,
University of Oklahoma, Norman, OK 73019, USA*

**E-mail: baer@nhn.ou.edu*

These lectures give an overview of aspects of missing E_T signatures from new physics at the LHC, along with their important connection to dark matter physics. Mostly, I will concentrate on supersymmetric (SUSY) sources of \cancel{E}_T , but will also mention Little Higgs models with T -parity (LHT) and universal extra dimensions (UED) models with KK -parity. Lecture 1 covers SUSY basics, model building and spectra computation. Lecture 2 addresses sparticle production and decay mechanisms at hadron colliders and event generation. Lecture 3 covers SUSY signatures at LHC, along with LHT and UED signatures for comparison. In Lecture 4, I address the dark matter connection, and how direct and indirect dark matter searches, along with LHC collider searches, may allow us to both discover and characterize dark matter in the next several years. Finally, the interesting scenario of Yukawa-unified SUSY is examined; this case works best if the dark matter turns out to be a mixture of axion/axino states, rather than neutralinos.

Keywords: Supersymmetry; collider physics; dark matter; missing transverse energy

1. Introduction: \cancel{E}_T collider signatures and the dark matter connection

I have been assigned the topic of discussing missing transverse energy signatures at hadron colliders, especially the CERN LHC, which should begin producing data in 2009. Every collider event— be they lepton-lepton, lepton-hadron or hadron-hadron interactions— will contain some amount of missing energy (\cancel{E}) just due to the fact that energy measurements are not perfectly precise. Hadronic events will usually contain more \cancel{E} than leptonic events since the energy resolution of hadronic calorimeters is not as precise as is electromagnetic resolution. In addition, collider detectors are imperfect devices, often containing un-instrumented regions, cracks, hot or dead

calorimeter cells, and only partial coverage of the 4π steradians surrounding the interaction region: always, an allowance must be made at least to allow the beam pipe to enter the detector. Also, missing energy can arise from cosmic rays entering the detector, or beam-gas collisions, multiple scattering etc.

At e^+e^- colliders, \cancel{E} can be directly measured since the incoming beam energies are well-known (aside from bremsstrahlung/beamstrahlung effects at very high energy e^+e^- colliders). At $p\bar{p}$ or pp colliders, the hard scattering events which are likely to produce new physics are initiated by quark-quark, quark-gluon, or gluon-gluon collisions, and the partonic constituents of the proton carry only a fraction of the beam energy. The proton constituents not participating in the hard scattering will carry an unknown fraction of beam energy into the un-instrumented or poorly instrumented forward region, so that for hadron colliders, only missing *transverse* energy (\cancel{E}_T) is meaningful. In these lectures, we will concentrate on pp colliders, in anticipation of the first forthcoming collisions at the CERN LHC.

Along with these imperfect detector effects, \cancel{E}_T can arise in Standard Model (SM) production processes wherein neutrinos are produced, either directly or via particle decays. For instance, the key signature for W boson production at colliders was the presence of a hard electron or muon balanced by missing energy coming from escaping neutrinos produced in $W^- \rightarrow \ell^- \bar{\nu}_\ell$ (or charge conjugate reaction) decay (here, $\ell = e, \mu$ or τ). In addition, neutrinos will be produced by semi-leptonic decays of heavy flavors and τ s, and indeed \cancel{E}_T was an integral component of $t\bar{t}$ production events followed by $t \rightarrow bW$ decays at the Fermilab Tevatron, and led to discovery of the top quark.

In these lectures, we will focus mainly on *new physics* reactions which lead to events containing large amounts of \cancel{E}_T . The major motivation nowadays that \cancel{E}_T signatures from new physics should appear at LHC comes from cosmology. A large array of data—coming from measurements of galactic rotation curves, galaxy cluster velocity profiles, gravitational lensing, hot gas in galaxy clusters, light element abundances in light of Big Bang nucleosynthesis, large scale structure simulations and measurements and especially measurements of anisotropies in the cosmic microwave background radiation (CMB)—all point to a consistent picture of a universe which is constructed of

- baryons: $\sim 4\%$
- dark matter: $\sim 21\%$
- dark energy: $\sim 75\%$

- ν s, γ s: a tiny fraction.

Thus, particles present in the SM of particle physics constitute only $\sim 4\%$ of the universe's energy budget, while the main portion is comprised of dark energy (DE) which causes an accelerating expansion of the universe and dark matter (DM). There is an ongoing program of experiments under way or under development which will probe the dark energy. The goal is to try to tell if DE comes from Einstein's cosmological constant (which theoretical prejudice says really ought to be there), or something quite different. Measurements focus on the parameters entering the dark energy equation of state.

For dark matter, there exist good reasons to believe that it will be connected to new physics arising at the weak scale: exactly the energy regime to be probed by the LHC. The density of dark matter is becoming known with increasing precision. The latest WMAP5 measurements¹ find

$$\Omega_{CDM}h^2 = 0.110 \pm 0.006 \quad (1)$$

where Ω_{CDM} is the cold DM density divided by the critical closure density of the universe ρ_c , and h is the scaled Hubble constant: $h = 0.73_{-0.03}^{+0.04}$. While the cosmic DM density is well-known, the identity of the DM particle(s) is completely unknown. Nevertheless, we do know some properties of the dark matter: it must have mass, it must be electrically neutral (non-interacting with light) and likely color neutral, and it must have a non-relativistic velocity profile, *i.e.* be what is termed *cold* dark matter (CDM). The reason it must be cold is that it must seed structure formation in the universe, *i.e.* it must clump. That means its velocity must be able to drop below its escape velocity; otherwise, it would disperse, and not seed structure formation. We already know of one form of dark matter: cosmic neutrinos. However, the SM neutrinos are so light that they must constitute *hot* dark matter.

The theoretical literature contains many possible candidate DM particles. A plot of some of these is shown in Fig. 1 (adapted from L. Roszkowski) in the mass vs. interaction cross section plane. Some of these candidates emerge from attempts to solve longstanding problems in particle physics. For instance, the axion arises from the Peccei-Quinn solution to the strong *CP* problem. The weakly interacting massive particles (WIMPs) frequently arise from models which attempt to explain the origin of electroweak symmetry breaking. WIMP dark matter candidates include the lightest neutralino of models with weak scale supersymmetry, while Kaluza-Klein photons arise in models with universal extra dimensions, and lightest *T*-odd particles arise in Little Higgs models with a conserved *T*-parity.

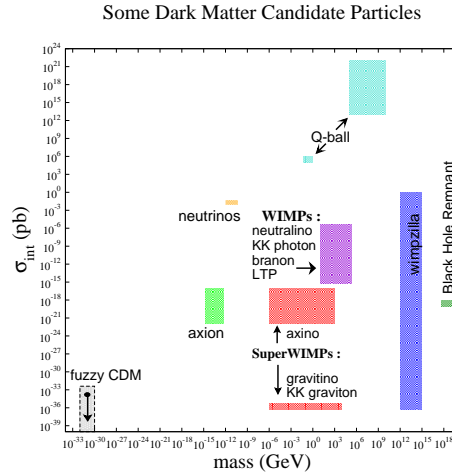


Fig. 1. *Dark matter candidates in the mass versus interaction strength plane, taken from Ref.:*² http://www.science.doe.gov/hep/hepap_reports.shtml. See also, *L. Roszkowski, Ref.*³

WIMP particles have an additional motivation, which has recently been coined the “WIMP miracle”.⁴ The idea here is to assume the existence of a dark matter particle which was once in thermal equilibrium at high temperatures in the early universe. The equilibrium abundance is easily calculated from thermodynamics and provides one boundary condition. As the universe expands and cools, the DM particle will drop out of thermal equilibrium (freeze-out); while DM will no longer be produced thermally, it can still annihilate away. The subsequent time evolution of the dark matter density is governed by the Boltzmann equation as formulated for the Friedman-Robertson-Walker universe:

$$dn/dt = -3Hn - \langle \sigma v_{rel} \rangle (n^2 - n_0^2) \quad (2)$$

wherein the $-3Hn$ terms gives rise to dilution due to the Hubble expansion, and the $\langle \sigma v_{rel} \rangle$ term involves the dark matter annihilation cross section. The Boltzmann equation is solved in various textbooks,⁵ and the solution is given approximately by

$$\Omega h^2 = \frac{s_0}{\rho_c/h^2} \left(\frac{45}{\pi g_*} \right)^{1/2} \frac{x_f}{M_{Pl}} \frac{1}{\langle \sigma v \rangle}, \quad (3)$$

where s_0 is the current entropy density, g_* is the effective degrees of freedom and x_f is the freeze-out temperature $\sim m_{\tilde{Z}_1}/20$. The quantities entering this

expression are unrelated to one another and several have large exponents. Filling in numerical values, they conspire to give

$$\Omega h^2 \sim \frac{0.1 \text{ pb}}{\langle \sigma v \rangle}, \quad (4)$$

so that in order to obtain the measured dark matter abundance $\Omega h^2 \sim 0.11$, we expect $\langle \sigma v \rangle$ to be a *weak scale sized cross section!*. Inputting a typical weak scale cross section,

$$\sigma = \frac{\alpha^2}{8\pi} \frac{1}{m^2} \quad (5)$$

and setting $\sigma \sim 1 \text{ pb}$, we find $m \sim 100 \text{ GeV}$! The lesson here is an important one: that the measured dark matter density is consistent with the annihilation cross section expected of a weakly interacting particle with *mass of order the weak scale*. This auspicious relation amongst dark matter density, annihilation cross section and particle mass is sometimes referred to as the *WIMP miracle*, and seemingly offers independent *astrophysical* evidence for new physics at or around the weak scale: in this case the new physics is associated with the cosmic density of dark matter. If such a WIMP particle exists, then it should be produced at large rates at the CERN LHC. Since it is dark matter, once produced in a collider experiment, it would escape normal detection. If produced in association with other SM particles (such as quarks and gluons), then it will carry away missing (transverse) energy, and will give rise to new physics signatures including jets plus \cancel{E}_T . It is this connection of weak scale physics and dark matter which makes the jets + \cancel{E}_T signature so important and exciting at the LHC.

2. Lecture 1: SUSY basics: model building and spectra calculation

2.1. The Wess-Zumino model

We begin with a toy model due to Wess and Zumino, from 1974.⁶ The model Lagrangian is given by

$$\mathcal{L} = \mathcal{L}_{\text{kin.}} + \mathcal{L}_{\text{mass}} \quad (6)$$

with

$$\begin{aligned} \mathcal{L}_{\text{kin.}} &= \frac{1}{2}(\partial_\mu A)^2 + \frac{1}{2}(\partial_{\mu\nu} B)^2 + \frac{i}{2}\bar{\psi}\not{\partial}\psi + \frac{1}{2}(F^2 + G^2) \\ \mathcal{L}_{\text{mass}} &= -m\left[\frac{1}{2}\bar{\psi}\psi - GA - FB\right], \end{aligned}$$

where A and B are real scalar fields, ψ is a 4-component Majorana spinor field and F and G are non-propagating *auxiliary* fields. The auxiliary fields may be eliminated from the Lagrangian via the Euler-Lagrange equations: $F = -mB$ and $G = -mA$.

But instead, impose the transformations

$$\begin{aligned} A &\rightarrow A + \delta A \text{ with } \delta A = i\bar{\alpha}\gamma_5\psi, \\ \delta B &= -\bar{\alpha}\psi, \\ \delta\psi &= -F\alpha + iG\gamma_5\alpha + \not{\partial}\gamma_5 A\alpha + i\not{\partial}B\alpha, \\ \delta F &= i\bar{\alpha}\not{\partial}\psi, \\ \delta G &= \bar{\alpha}\gamma_5\not{\partial}\psi. \end{aligned}$$

Note that the transformation mixes bosonic and fermionic fields. It is called a *supersymmetry* transformation. Using Majorana bilinear re-arrangements (such as $\bar{\psi}\chi = -\bar{\chi}\psi$), the product rule $\partial_\mu(f \cdot g) = \partial_\mu f \cdot g + f \cdot \partial_\mu g$ and some algebra, we find that $\mathcal{L} \rightarrow \mathcal{L} + \delta\mathcal{L}$ with

$$\begin{aligned} \delta\mathcal{L}_{\text{kin}} &= \partial^\mu \left(-\frac{1}{2}\bar{\alpha}\gamma_\mu\not{\partial}B\psi + \frac{i}{2}\bar{\alpha}\gamma_5\gamma_\mu\not{\partial}A\psi + \frac{i}{2}F\bar{\alpha}\gamma_\mu\psi + \frac{1}{2}G\bar{\alpha}\gamma_5\gamma_\mu\psi \right), \\ \delta\mathcal{L}_{\text{mass}} &= \partial^\mu (mA\bar{\alpha}\gamma_5\gamma_\mu\psi + imB\bar{\alpha}\gamma_\mu\psi). \end{aligned}$$

Since the Lagrangian changes by a total derivative, the *action* $S = \int \mathcal{L}d^4x$ is invariant! (owing to Gauss' law in 4-d $\int_V d^4x\partial_\mu\Lambda^\mu = \int_{\partial V} d\sigma\Lambda^\mu n_\mu$). Under supersymmetry transformations, the Lagrangian always transforms into a total derivative, leaving the action invariant.

The Wess-Zumino (WZ) model as presented in 1974 exhibited a qualitatively new type of symmetry transformation with astonishing properties: one being that the usual quantum field theory quadratic divergences associated with scalar fields all cancel! Theories with this sort of property might allow for a solution of the so-called ‘‘gauge hierarchy problem’’ of grand unified theories (GUTs).

2.2. Superfield formalism

While the WZ model was very compelling, it was constructed by hand, and offered no insight into how to construct general supersymmetric models. A short while later, Salam and Strathdee⁷ developed the superfield formalism, which did provide rules for general SUSY model building. They first expanded the usual four-component spacetime x^μ to *superspace*: $x^\mu \rightarrow (x^\mu, \theta_a)$, where θ_a ($a = 1-4$) represents four *anti-commuting* (Grassmann valued) dimensions arranged as a Majorana spinor. Then they intro-

duced *general* superfields:

$$\begin{aligned} \hat{\Phi}(x, \theta) = & \mathcal{S} - i\sqrt{2}\bar{\theta}\gamma_5\psi - \frac{i}{2}(\bar{\theta}\gamma_5\theta)\mathcal{M} + \frac{1}{2}(\bar{\theta}\theta)\mathcal{N} + \frac{1}{2}(\bar{\theta}\gamma_5\gamma_\mu\theta)V^\mu \\ & + i(\bar{\theta}\gamma_5\theta)[\bar{\theta}(\lambda + \frac{i}{\sqrt{2}}\not{\partial}\psi)] - \frac{1}{4}(\bar{\theta}\gamma_5\theta)^2[\mathcal{D} - \frac{1}{2}\square\mathcal{S}], \end{aligned}$$

left chiral scalar superfields (LCSSF):

$$\hat{\mathcal{S}}_L(x, \theta) = \mathcal{S}(\hat{x}) + i\sqrt{2}\bar{\theta}\psi_L(\hat{x}) + i\bar{\theta}\theta_L\mathcal{F}(\hat{x}) \quad (7)$$

(where $\hat{x}_\mu = x_\mu + \frac{i}{2}\bar{\theta}\gamma_5\gamma_\mu\theta$) and right chiral scalar superfields (RCSSF):

$$\hat{\mathcal{S}}_R(x, \theta) = \mathcal{S}(\hat{x}^\dagger) - i\sqrt{2}\bar{\theta}\psi_R(\hat{x}^\dagger) - i\bar{\theta}\theta_R\mathcal{F}(\hat{x}^\dagger). \quad (8)$$

The multiplication table for superfields is as follows:

- $LCSSF \times LCSSF = LCSSF$
- $RCSSF \times RCSSF = RCSSF$
- $LCSSF \times RCSSF =$ a general superfield.

Moreover, under a supersymmetry transformation, the D -term of a general superfield and the F term of a LCSSF or a RCSSF always transforms into a total derivative.

This last observation gave the key insight allowing for construction of general supersymmetric models. The superpotential \hat{f} is a function of LCSSFs only, and hence by the multiplication table above is itself a LCSSF. Its F term transforms into a total derivative under SUSY, and hence is a candidate Lagrangian. Also, the Kahler potential K is introduced: it is a function of products of RCSSFs times LCSSFs: it is therefore a general superfield and its D -term transforms into a total derivative under SUSY, and hence its D -term is a candidate Lagrangian. The choice $K = \sum_{fields} \hat{\mathcal{S}}^\dagger \hat{\mathcal{S}}$ is completely general for a renormalizable theory. Augmenting the above superfields with *gauge* superfields (ones containing spin-1 gauge bosons and spin- $\frac{1}{2}$ gauginos all transforming under the adjoint representation) allows one to construct locally gauge invariant, renormalizable field theories which are also invariant under SUSY transformations.

A Master Lagrangian can then be constructed. Its form is given in Ch. 5 of Ref.⁸ It allows for a recipe for SUSY model building:

- select the gauge group (simple or direct product),
- select the matter and Higgs representations,
- write down a superpotential (gauge invariant and renormalizable),
- plug all terms into the Master Lagrangian, calculate the physical states and Feynman rules, and you are good to go!

2.3. Minimal Supersymmetric Standard Model (MSSM)

The superfield formalism^{8–10} allows for the construction of a supersymmetric version of the Standard Model, known as the Minimal Supersymmetric Standard Model, or MSSM. For each quark and lepton of the SM, the MSSM necessarily includes spin-0 superpartners \tilde{q}_L and \tilde{q}_R along with $\tilde{\ell}_L$ and $\tilde{\ell}_R$, whose gauge quantum numbers are fixed to be the known gauge quantum numbers of the corresponding SM fermions. Thus, for example, the right-handed up quark scalar (usually denoted by \tilde{u}_R) is a color-triplet, weak isosinglet with the same weak hypercharge $4/3$ as the right-handed up-quark. The MSSM thus includes a plethora of new scalar states: \tilde{e}_L , \tilde{e}_R , $\tilde{\nu}_{eL}$, \tilde{u}_L , \tilde{u}_R , \tilde{d}_L , \tilde{d}_R in the first generation, together with analogous states for the other two generations. Spin-zero *squark* partners of quarks with large Yukawa couplings undergo left-right mixing: thus, the \tilde{t}_L and \tilde{t}_R states mix to form mass eigenstates – \tilde{t}_1 and \tilde{t}_2 – ordered from lowest to highest mass.

The spin-0 Higgs bosons are embedded in Higgs superfields, so that the MSSM also includes spin- $\frac{1}{2}$ higgsinos. Unlike in the SM, the same Higgs doublet cannot give a mass to both up- and down- type fermions without catastrophically breaking the underlying supersymmetry. Thus the MSSM includes two Higgs doublets instead of one as in the SM. This gives rise to a richer spectrum of physical Higgs particles, including neutral light h and heavy H scalars, a pseudoscalar A and a pair of charged Higgs bosons H^\pm .

The gauge sector of the MSSM contains gauge bosons along with spin-half gauginos in the adjoint representation of the gauge group: thus, along with eight colored gluons, the MSSM contains eight colored spin- $\frac{1}{2}$ gluinos. Upon electroweak symmetry breaking, the four gauginos of $SU(2)_L \times U(1)_Y$ mix (just as the $SU(2)_L$ and $U(1)_Y$ gauge bosons mix) amongst themselves *and* the higgsinos, to form charginos – \tilde{W}_1^\pm and \tilde{W}_2^\pm – and neutralinos – \tilde{Z}_1 , \tilde{Z}_2 , \tilde{Z}_3 and \tilde{Z}_4 . The \tilde{Z}_1 state, the lightest neutralino, is often the lightest supersymmetric particle (LSP), and turns out to be an excellent WIMP candidate for CDM in the universe.

If nature is perfectly supersymmetric, then the *spin-0 superpartners would have exactly the same mass* as the corresponding fermions. Charged spin-0 partners of the electron with a mass of 0.51 MeV could not have evaded experimental detection. Their non-observation leads us to conclude that SUSY must be a *broken* symmetry. In the MSSM, SUSY is broken *explicitly* by including so-called soft SUSY breaking (SSB) terms in the Lagrangian. The SSB terms preserve the desirable features of SUSY, such as the stabilization of the scalar sector in the presence of radiative correc-

tions, while lifting the superpartner masses in accord with what is necessary from experiment. It is important to note that the equality of dimensionless couplings between particles and their superpartners is still preserved (modulo small effects of radiative corrections): in particular, phenomenologically important gauge interactions of superpartners and the corresponding interactions of gauginos remain (largely) unaffected by the SSB terms.

2.4. *Supergravity*

The addition of the SSB Lagrangian terms may seem *ad-hoc* and ugly. It would be elegant if instead supersymmetry could be spontaneously broken. But it was recognized in the early to mid-1980's that models where global SUSY is spontaneously broken at the weak scale ran into serious difficulties. The situation is very different if we elevate SUSY from a global symmetry to a *local* one. In local SUSY, we are *forced to include the graviton/gravitino super-multiplet* into the theory, in much the same way that we have to include spin-1 gauge fields to maintain local gauge invariance of Yang-Mills theories. Theories with local SUSY are known as *supergravity* (SUGRA) theories because they are supersymmetric and necessarily include gravity. Moreover, the gravitational sector of the theory reduces to general relativity in the classical limit. Within the framework of SUGRA, it is possible to add an additional sector whose dynamics spontaneously breaks SUSY but which interacts with SM particles and their superpartners only via gravity (the so-called hidden sector). The spontaneous breakdown of supersymmetry results in a mass for the gravitino in the same way that in local gauge theories gauge bosons acquire mass by the Higgs mechanism. This is, therefore, referred to as the *super-Higgs mechanism*. The remarkable thing is that because of the gravitational coupling between the hidden and the MSSM sectors, the effects of spontaneous supersymmetry breaking in the hidden sector are conveyed to the MSSM sector, and (provided the SUSY-breaking scale in the hidden sector is appropriately chosen) weak scale SSB terms that lift the undesirable degeneracies between the masses of SM particles and their superpartners are automatically induced. Indeed, in the limit where $M_{\text{Pl}} \rightarrow \infty$ (keeping the gravitino mass fixed), we recover a global SUSY theory along with the desired SSB terms! The gravitino typically has a weak scale mass and in many cases decouples from collider experiments because of its tiny gravitational couplings. For reasons that we cannot discuss here, these locally supersymmetric models are free⁸⁻¹⁰ of many of the difficulties that plague globally supersymmetric models.

2.5. *SUGRA GUTs*

Motivated by the successful unification of gauge couplings at a scale $M_{\text{GUT}} \sim 2 \times 10^{16}$ GeV in the MSSM, we are led to construct a grand unified theory (GUT) based on local supersymmetry. In this case, the theory renormalized at $Q = M_{\text{GUT}}$ contains just one gaugino mass parameter $m_{1/2}$. Renormalization effects then split the physical gaugino masses in the same way the measured values of the gauge couplings arise from a single unified GUT scale gauge coupling. In general, supergravity models give rise to complicated mass matrices for the scalar superpartners of quarks and leptons, with concomitant flavor violation beyond acceptable levels. However, in models with *universal* soft SUSY breaking terms, a super-GIM mechanism suppresses flavor violating processes.¹¹ In what has come to be known as the minimal supergravity (mSUGRA) model, a universal scalar mass m_0 and also a universal SSB scalar coupling A_0 are assumed to exist at a high scale $Q \sim M_{\text{GUT}} - M_{\text{Pl}}$. The physical masses of squarks and sleptons are split after renormalization, and can be calculated using renormalization group techniques. Typically, in the mSUGRA model, we have $m_{\tilde{q}} \gtrsim m_{\tilde{l}_L} \gtrsim m_{\tilde{l}_R}$. Although the Higgs scalar mass parameters also start off at the common value m_0 at the high scale, the large value of the top quark Yukawa coupling drives the corresponding squared mass parameter to negative values and EWSB is *radiatively broken*. Within this framework, the masses and couplings required for phenomenology are fixed by just a handful of parameters which are usually taken to be,

$$m_0, m_{1/2}, A_0, \tan\beta, \text{ and } \text{sign}(\mu). \quad (9)$$

Here, $\tan\beta$ is the ratio of the vacuum expectation values of the Higgs fields that give masses to up and down type fermions, and μ is the supersymmetric higgsino mass parameter whose magnitude is fixed to reproduce the measured value of M_Z . If all parameters are real, then potentially large *CP*-violating effects are suppressed as well. Computer codes such as Isajet, SuSpect, SoftSUSY and Spheno that calculate the full spectrum of sparticle and Higgs boson masses are publicly available.¹²

2.6. *Some realistic SUSY models*

The mSUGRA model (sometimes referred to as the constrained MSSM or CMSSM) serves as a paradigm for many SUSY phenomenological analyses. However, it is important to remember that it is based on many assumptions that can be tested in future collider experiments but which

may prove to be incorrect. For instance, in many GUT theories, it is common to get *non-universal* SSB parameters. In addition, there are other messenger mechanisms besides gravity. In gauge-mediated SUSY breaking models (GMSB),¹³ a special messenger sector is included, so gravitinos may be much lighter than all other sparticles, with implications for both collider physics and cosmology. In anomaly-mediated SUSY breaking (AMSB) models,¹⁴ gravitational anomalies induce SSB terms, and the gravitino can be much heavier than the weak scale. There are yet other models¹⁵ where SSB parameters get comparable contributions from gravity-mediated as well as from anomaly-mediated sources, and very recently, also from gauge-mediation.¹⁶ The pattern of superpartner masses is sensitive to the mediation-mechanism, so that we can expect collider experiments to reveal which of the various mechanisms that have been proposed are actually realized in nature. We also mention that in both the GMSB and AMSB models, it is somewhat less natural (but still possible!) to obtain the required amount of SUSY dark matter in the Universe. Although these are all viable scenarios, they have not been as well scrutinized as the mSUGRA model.

3. Lecture 2: Sparticle production, decay and event generation

3.1. *The role of the CERN Large Hadron Collider*

The CERN Large Hadron Collider (LHC) turned on briefly in 2008 before an electrical mis-connection caused a helium leak, and a shut-down until mid-2009. The LHC is a pp collider, expected to operate ultimately at center-of-mass energy $\sqrt{s} = 14$ TeV. Since protons are not fundamental particles, we may think instead of LHC as being a quark-gluon collider, where the quark and gluon constituents of the proton that undergo hard strong or electroweak scatterings only carry typically a small fraction of the proton energy.

For the hadronic reaction

$$A + B \rightarrow c + d + X, \quad (10)$$

where A and B are hadrons, c and d might be superpartners, and X is associated hadronic debris, we are really interested in the subprocess reaction

$$a + b \rightarrow c + d, \quad (11)$$

where a is a partonic constituent of hadron A , and b is a partonic constituent of hadron B . The SM or MSSM or whatever effective theory we are working

in provides us with the Feynman rules to calculate the subprocess cross-section $\hat{\sigma}(ab \rightarrow cd)$. To find the total hadron-hadron cross section, we must convolute the subprocess cross section with the *parton distribution functions* $f_{a/A}(x_a, Q^2)$ which gives the probability to find parton a in hadron A with momentum fraction x_a at energy-squared scale Q^2 . Thus, we have

$$d\sigma(AB \rightarrow cdX) = \sum_{a,b} \int_0^1 dx_a \int_0^1 dx_b f_{a/A}(x_a, Q^2) f_{b/B}(x_b, Q^2) d\hat{\sigma}(ab \rightarrow cd). \quad (12)$$

where the sum extends over all initial partons a and b whose collisions produce the final state particles c and d . The parton-parton center-of-mass energy-squared $\hat{s} = x_a x_b s$ which enters the hard scattering is only a small fraction of the proton-proton center-of-mass energy-squared s . Thus, to explore the TeV scale, a hadron-hadron collider of tens of TeV is indeed needed!

Around the 17 mile circumference LHC ring are situated four experiments: Atlas, CMS, LHC-B and Alice. Atlas and CMS are all-purpose detectors designed to detect almost all the energy emitted in hard scattering reactions. They will play a central role in the search for new physics at the LHC, and the search for dark matter production in the LHC environment.

3.2. Cross section calculations for the LHC

As noted above, if a perturbative model for new physics is available, then the relativistic-quantum mechanical amplitude \mathcal{M} for the relevant scattering sub-process may be calculated, usually at a low order in perturbation theory. The probability for scattering is given by the square of the (complex) scattering amplitude $\mathcal{M}\mathcal{M}^\dagger$, and can often be expressed as a function of dot products of the external leg momenta entering the diagrams, after summing and averaging over spins and colors. Nowadays, several computer programs—such as CalcHEP, CompHEP and MadGraph—are available to automatically do tree level calculations of various $2 \rightarrow n$ processes.

To gain the parton level scattering cross section, one must multiply by suitable phase space factors and divide by the flux factor. The phase space integrals for simple sub-processes may be done analytically. More often, the final integrals are done using Monte Carlo (MC) techniques, which efficiently allow integration over multi-body phase space. The MC technique, wherein random integration variables are generated computationally, and summed over, actually allows for a *simulation* of the scattering process. This can allow one to impose cuts, or simulate detectors, to gain a more

exact correspondence to the experimental environment.

3.3. Sparticle production at the LHC

Direct production of neutralino dark matter at the LHC ($pp \rightarrow \tilde{Z}_1 \tilde{Z}_1 X$, where X again stands for assorted hadronic debris) is of little interest since the high p_T final state particles all escape the detector, and there is little if anything to trigger an event record. Detectable events come from the production of the heavier superpartners, which in turn decay via a multi-step cascade which ends in the stable lightest SUSY particle (LSP).

In many SUSY models, the strongly interacting squarks and/or gluinos are among the heaviest states. Unless these are extremely heavy, they will have large production cross sections at the LHC. Strong interaction production mechanisms for their production include, 1. gluino pair production $\tilde{g}\tilde{g}$, 2. squark pair production $\tilde{q}\tilde{q}$ and 3. squark-gluino associated production $\tilde{q}\tilde{g}$. Note here that the reactions involving squarks include a huge number of subprocess reactions to cover the many flavors, types (left- and right-), and also the anti-squarks. The various possibilities each have different angular dependence in the production cross sections,¹⁷ and the different flavors/types of squarks each have different decay modes.¹⁸ These all have to be kept track of in order to obtain a reliable picture of the implications of SUSY in the LHC detector environment. Squarks and gluinos can also be produced in association with charginos and neutralinos.¹⁹ Associated gluino production occurs via squark exchange in the t or u channels and is suppressed if squarks are very heavy.

If colored particles are very heavy, then electroweak production of charginos and neutralinos may be the dominant sparticle production mechanism at the LHC. The most important processes are pair production of charginos, $\tilde{W}_i^\pm \tilde{W}_j^\mp$ where $i, j = 1, 2$, and chargino-neutralino production, $\tilde{W}_i^\pm \tilde{Z}_j$, with $i = 1, 2$ and $j = 1 - 4$. In models with unified GUT scale gaugino masses and large $|\mu|$, $Z\tilde{W}_1\tilde{W}_1$ and $W\tilde{Z}_2\tilde{W}_1$ couplings are large so that $\tilde{W}_1\tilde{W}_1$ and $\tilde{W}_1\tilde{Z}_2$ production occurs at significant rates. The latter process can lead to the gold-plated trilepton signature at the LHC.²⁰ Neutralino pair production ($pp \rightarrow \tilde{Z}_i \tilde{Z}_j X$ where $i, j = 1 - 4$) is also possible. This reaction occurs at low rates at the LHC unless $|\mu| \simeq M_{1,2}$ (as in the case of mixed higgsino dark matter (MHDM)). Finally, we mention slepton pair production: $\tilde{\ell}^+ \tilde{\ell}^-$, $\tilde{\nu}_\ell \tilde{\ell}$ and $\tilde{\nu}_\ell \tilde{\nu}_\ell$, which can give detectable dilepton signals if $m_{\tilde{\ell}} \lesssim 300$ GeV.²¹

In Fig. 2 we show various sparticle production cross sections at the LHC as a function of $m_{\tilde{g}}$. Strong interaction production mechanisms dominate

at low mass, while electroweak processes dominate at high mass. The associated production mechanisms are never dominant. The expected LHC integrated luminosity in the first year of running is expected to be around 0.1 fb^{-1} , while several tens of fb^{-1} of data is expected to be recorded in the first several years of operation. The ultimate goal is to accumulate around $500\text{-}1000 \text{ fb}^{-1}$, corresponding to $10^5 - 10^6$ SUSY events for $m_{\tilde{g}} \sim 1 \text{ TeV}$.

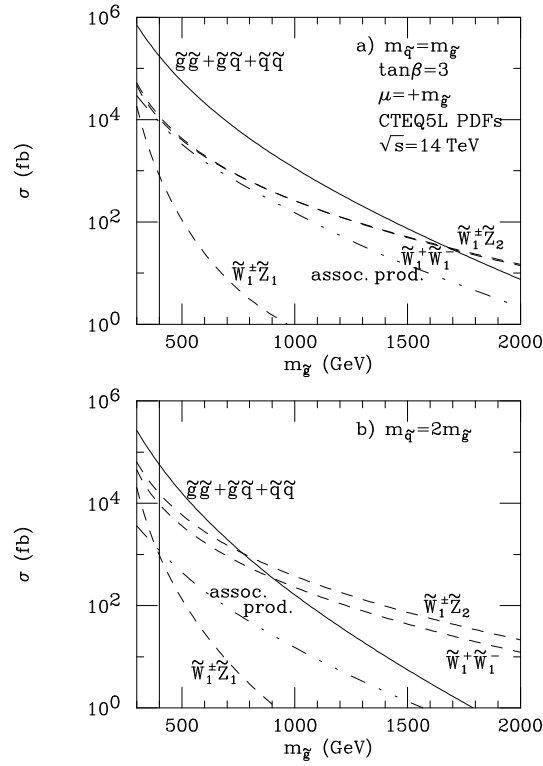


Fig. 2. Cross sections for production of various sparticles at the LHC. Gaugino mass unification is assumed.

3.4. Sparticle cascade decays

In R -parity conserving SUSY models, sparticles decay to lighter sparticles until the decay terminates in the LSP.¹⁸ Frequently, the direct decay to the LSP is either forbidden or occurs with only a small branching fraction. Since gravitational interactions are negligible, gluinos can only decay via

$\tilde{g} \rightarrow q\tilde{q}$, where the q and \tilde{q} can be of any flavor or type. If two body decay modes are closed, the squark will be virtual, and the gluino will decay via three body modes $\tilde{g} \rightarrow q\tilde{q}\tilde{Z}_i$, $q\tilde{q}'\tilde{W}_j$. If squarks are degenerate, and Yukawa coupling effects negligible, three-body decays to the wino-like chargino and neutralino usually have larger branching fractions on account of the larger gauge coupling. If $|\mu| < M_2$, gluinos and squarks may thus decay most of the time to the heavier charginos and neutralinos, resulting in lengthy cascade decay chains at the LHC.

Squarks decay always to two-body modes: $\tilde{q} \rightarrow q\tilde{g}$ if it is kinematically allowed, or $\tilde{q}_L \rightarrow q'\tilde{W}_i$, $q\tilde{Z}_j$, while $\tilde{q}_R \rightarrow q\tilde{Z}_j$ only, since right-squarks do not couple to charginos. Sleptons do not have strong interactions so cannot decay to gluinos. Their electroweak decays are similar to corresponding decays of squarks $\tilde{\ell}_L \rightarrow \ell'\tilde{W}_i$, $\ell\tilde{Z}_j$ while $\tilde{\ell}_R \rightarrow \ell\tilde{Z}_j$ only.

Charginos may decay via two-body modes: $\tilde{W}_i \rightarrow W\tilde{Z}_j$, $\tilde{\ell}\nu_\ell$, $\ell\tilde{\nu}_\ell$, $Z\tilde{W}_j$ or even to $\phi\tilde{W}_j$ or $H^-\tilde{Z}_j$, where $\phi = h, H, A$. If two-body modes are inaccessible, then three-body decays dominate: $\tilde{W}_i \rightarrow \tilde{Z}_j f\tilde{f}'$, where f and f' are SM fermions which couple to the W . Frequently, the decay amplitude is dominated by the virtual W so that the three-body decays of \tilde{W}_1 have the same branching fractions as those of the W . Neutralinos decay via $\tilde{Z}_i \rightarrow W\tilde{W}_j$, $H^+\tilde{W}_j$, $Z\tilde{Z}_j$, $\phi\tilde{Z}_j$ or $f\tilde{f}$. If two body neutralino decays are closed, then $\tilde{Z}_i \rightarrow \tilde{Z}_j f\tilde{f}$, where f are the SM fermions. In some models, the branching fraction for radiative decays $\tilde{Z}_i \rightarrow \tilde{Z}_j\gamma$ (that only occurs at the one-loop level) may be significant.²² The cascade decay modes of neutralinos depend sensitively on model parameters.²³

If $\tan\beta$ is large, then b and τ Yukawa coupling effects become important, enhancing three body decays of \tilde{g} , \tilde{W}_i and \tilde{Z}_j to third generation fermions.²⁴ For very large values of $\tan\beta$ these decays can even dominate, resulting in large rates for b -jet and τ -jet production in SUSY events.²⁵

Finally, the various Higgs bosons can be produced both directly and via sparticle cascades at the LHC.²⁶ Indeed, it may be possible that h is first discovered in SUSY events because in a sample of events enriched for SUSY, it is possible to identify h via its dominant $h \rightarrow b\bar{b}$ decays rather than via its sub-dominant decay modes, as required for conventional searches.²⁶ The heavier Higgs bosons decay to a variety of SM modes, but also to SUSY particles if these latter decays are kinematically allowed, leading to novel signatures such as $H, A \rightarrow \tilde{Z}_2\tilde{Z}_2 \rightarrow 4\ell + \cancel{E}_T$.²⁷

The cascade decays terminate in the LSP. In the case of a \tilde{Z}_1 LSP, the \tilde{Z}_1 is a DM candidate, and leaves its imprint via \cancel{E}_T . In the case of a weak scale \tilde{G} or \tilde{a} LSP, then \tilde{Z}_1 will decay as $\tilde{Z}_1 \rightarrow \gamma\tilde{G}$ or $\gamma\tilde{a}$. In these cases,

the \tilde{Z}_1 lifetime is long enough that it decays outside the detector, so one still expects large \cancel{E}_T in the collider events. An exception arises for the case of super-light gravitinos (with masses in the eV to keV range) that are possible in GMSB models: see (15). Then, the decay may take place inside the detector, possibly with a large vertex separation. It is also possible that the NLSP is charged and quasi-stable, in which case collider events may include highly ionizing tracks instead of, or in addition to, \cancel{E}_T .

The decay branching fractions depend on the entire spectrum of SUSY particle masses and their mixings. They are pre-programmed in several codes: Isajet,²⁸ SDECAY²⁹ and Spheno.³⁰

3.5. *Event generation for LHC*

Once sparticle production cross sections and decay branching fractions have been computed, it is useful to embed these into event generator programs to simulate what SUSY collider events will look like at LHC. There are several steps involved:

- Calculate all sparticle pair production cross sections. Once all initial and final states are accounted for, this involves over a thousand individual subprocess reactions. In event generation, a particular reaction is selected on a probabilistic basis, with a weight proportional to its differential cross-section.
- Sparticle decays are selected probabilistically into all the allowed modes in proportion to the corresponding branching fractions.
- Initial and final state quark and gluon radiation are usually dealt with using the parton shower (PS) algorithm, which allows for probabilistic parton emission based on approximate collinear QCD emission matrix elements, but exact kinematics. The PS is also applied at each step of the cascade decays, which may lead to additional jet production in SUSY collider events.
- A hadronization algorithm provides a model for turning various quarks and gluons into mesons and baryons. Unstable hadrons must be further decayed.
- The beam remnants – proton constituents not taking part in the hard scattering – must be showered and hadronized, usually with an independent algorithm, so that energy deposition in the forward detector region may be reliably calculated.

At this stage, the output of an event generator program is a listing of particle types and their associated four-vectors. The resulting event can

then be interfaced with detector simulation programs to model what the actual events containing DM will look like in the environment of a collider detector.

Several programs are available, including Isajet,²⁸ Pythia,³¹ Herwig³² and Sherpa.³³ Other programs such as MadEvent,³⁴ CompHEP/CalcHEP³⁵ and Whizard³⁶ can generate various $2 \rightarrow n$ processes including SUSY particles. The output of these programs may then be used as input to Pythia or Herwig for showering and hadronization. Likewise, parton level Isajet SUSY production followed by cascade decays can be input to Pythia and Herwig via the Les Houches Event format.³⁷

4. Lecture 3: SUSY, LHT and UED signatures at the LHC

4.1. Signatures for SUSY particle production

Unless colored sparticles are very heavy, the SUSY events at the LHC mainly result in gluino and squark production, followed by their possibly lengthy cascade decays. These events, therefore, typically contain very hard jets (from the primary decay of the squark and/or gluino) together with other jets and isolated electrons, muons and taus (identified as narrow one- and three-prong jets), and sometimes also photons, from the decays of secondary charginos and neutralinos, along with \cancel{E}_T that arises from the escaping dark matter particles (as well as from neutrinos). In models with a superlight gravitino, there may also be additional isolated photons, leptons or jets from the decay of the NLSP. The relative rates for various n -jet + m -lepton + k -photon + \cancel{E}_T event topologies is sensitive to the model as well as to the parameter values, and so provide a useful handle for phenomenological analyses.

Within the SM, the physics background to the classic *jets*+ \cancel{E}_T signal comes from neutrinos escaping the detector. Thus, the dominant SM backgrounds come from $W + jets$ and $Z + jets$ production, $t\bar{t}$ production, QCD multijet production (including $b\bar{b}$ and $c\bar{c}$ production), WW , WZ , ZZ production plus a variety of $2 \rightarrow n$ processes which are not usually included in event generators. These latter would include processes such as $t\bar{t}t$, $t\bar{t}b$, $t\bar{t}W$, WWW , WWZ production, *etc.* Decays of electroweak gauge bosons and the t -quark are the main source of isolated leptons in the SM. Various additional effects— uninstrumented regions, energy mis-measurement, cosmic rays, beam-gas events— can also lead to \cancel{E}_T events.

In contrast to the SM, SUSY events naturally tend to have large jet multiplicities and frequently an observable rate for high multiplicity lepton

events with large \cancel{E}_T . Thus, if one plots signal and background versus multiplicity of any of these quantities, as one steps out to large multiplicity, the expected SUSY events should increase in importance, and even dominate the high multiplicity channels in some cases. This is especially true of isolated multi-lepton signatures, and in fact it is convenient to classify SUSY signal according to lepton multiplicity:³⁸

- zero lepton $+jets+\cancel{E}_T$ events,
- one lepton $+jets+\cancel{E}_T$ events,
- two opposite sign leptons $+jets+\cancel{E}_T$ events (OS),
 - same-flavor (OSSF),
 - different flavor (OSDF),
- two same sign leptons $+jets+\cancel{E}_T$ events (SS),
- three leptons $+jets+\cancel{E}_T$ events (3ℓ),
- four (or more) leptons $+jets+\cancel{E}_T$ events (4ℓ).

4.2. LHC reach for SUSY

Event generators, together with detector simulation programs can be used to project the SUSY discovery reach of the LHC. Given a specific model, one may first generate a grid of points that samples the parameter (sub)space where signal rates are expected to vary significantly. A large number of SUSY collider events can then be generated at every point on the grid along with the various SM backgrounds to the SUSY signal mentioned above. Next, these signal and background events are passed through a detector simulation program and a jet-finding algorithm is implemented to determine the number of jets per event above some $E_T(jet)$ threshold (usually taken to be $E_T(jet) > 50 - 100$ GeV for LHC). Finally, *analysis cuts* are imposed which are designed to reject mainly SM BG while retaining the signal. These cuts may include both topological and kinematic selection criteria. For observability with an assumed integrated luminosity, we require that the signal exceed the chance 5 standard deviation upward fluctuation of the background, together with a minimum value of ($\sim 25\%$) the signal to background ratio, to allow for the fact that the background is not perfectly known. For lower sparticle masses, softer kinematic cuts are used, but for high sparticle masses, the lower cross sections but higher energy release demand hard cuts to optimize signal over background.

In Fig. 3, we illustrate the SUSY reach of the LHC within the mSUGRA model assuming an integrated luminosity of 100 fb^{-1} . We show the result in the $m_0 - m_{1/2}$ plane, taking $A_0 = 0$, $\tan\beta = 10$ and $\mu > 0$. The signal

is observable over background in the corresponding topology below the corresponding curve. We note the following.

- (1) Unless sparticles are very heavy, there is an observable signal in several different event topologies. This will help add confidence that one is actually seeing new physics, and may help to sort out the production and decay mechanisms.
- (2) The reach at low m_0 extends to $m_{1/2} \sim 1400$ GeV. This corresponds to a reach for $m_{\tilde{q}} \sim m_{\tilde{g}} \sim 3.1$ TeV.
- (3) At large m_0 , squarks and sleptons are in the 4 – 5 TeV range, and are too heavy to be produced at significant rates at LHC. Here, the reach comes mainly from just gluino pair production. In this range, the LHC reach is up to $m_{1/2} \sim 700$ GeV, corresponding to a reach in $m_{\tilde{g}}$ of about 1.8 TeV, and may be extended by $\sim 15\text{-}20\%$ by b -jet tagging.³⁹

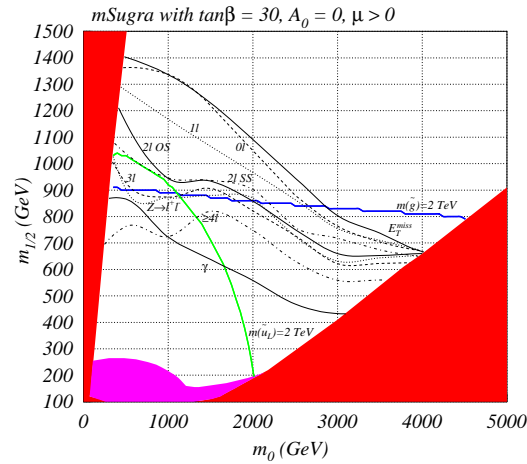


Fig. 3. The 100 fb^{-1} reach of LHC for SUSY in the $mSUGRA$ model. For each event topology, the signal is observable below the corresponding contour.

In Fig. 4 we can see a comparison of the LHC reach (notice that it is insensitive to $\tan\beta$ and $\text{sign}(\mu)$) with that of the Tevatron (for clean 3ℓ events with 10 fb^{-1}), and the proposed e^+e^- International Linear Collider (ILC), with $\sqrt{s} = 0.5$ or 1 TeV along with various dark matter direct detection (DD) and indirect detection (ID) search experiments. We remark that:

- While LHC can cover most of the relic density allowed region, the HB/FP region emerges far beyond the LHC reach.
- As will be discussed, the DD and ID experiments have the greatest sensitivity in the HB/FP region where the neutralino is MHDM. In this sense, DD and ID experiments *complement* LHC searches for SUSY.
- The ILC reach is everywhere lower than LHC, except in the HB/FP region. In this region, while gluinos and squarks can be extremely heavy, the μ parameter is small, leading to a relatively light spectrum of charginos and neutralinos. These are not detectable at the LHC because the visible decay products are too soft. However, since chargino pair production is detectable at ILC even if the energy release in chargino decays is small, the ILC reach extends beyond LHC in this region.⁴⁰

Finally, we note here that while the results presented above are for the LHC reach in the mSUGRA model, the LHC reach (measured in terms of $m_{\tilde{g}}$ and $m_{\tilde{q}}$) tends to be relatively insensitive to the details of the model chosen, as long as gluino and squark production followed by cascade decays to the DM particle occur.

4.3. *Early discovery of SUSY at LHC without \cancel{E}_T*

The classic signature for SUSY at hadron colliders is the presence of jets, isolated leptons and especially large \cancel{E}_T . However, in the early period of LHC running, \cancel{E}_T may be very difficult to measure reliably. In a real detector, there will be calorimetry calibration issues, dead or uninstrumented regions, “hot” cells, cosmic ray events, beam-gas collisions: all of these contribute to \cancel{E}_T events, in addition to SM backgrounds and possibly new physics. As learned from Tevatron experiments, a reliable measurement of \cancel{E}_T requires knowledge of the complete detector, and that may well take some time—possibly over a year—after start-up.

Can LHC search for SUSY even if \cancel{E}_T searches are not viable? The answer seems to be yes, as long as lepton isolation cuts are possible. In Ref.⁴¹ it was shown that requiring events with ≥ 4 jets plus a *high multiplicity* of isolated leptons: SS, OSSF, OSDF, 3ℓ , \dots would allow one to severely reduce SM background while maintaining large enough signal rates. It is claimed that an LHC reach of $m_{\tilde{g}} \sim 750$ GeV is possible with just 0.1 fb^{-1} of integrated luminosity, *without* using an \cancel{E}_T cut, by requiring events with ≥ 3 isolated leptons (e s or μ s).

In addition, reliable electron identification may also be an issue in early LHC running. The problem here is differentiating the electron’s EM shower

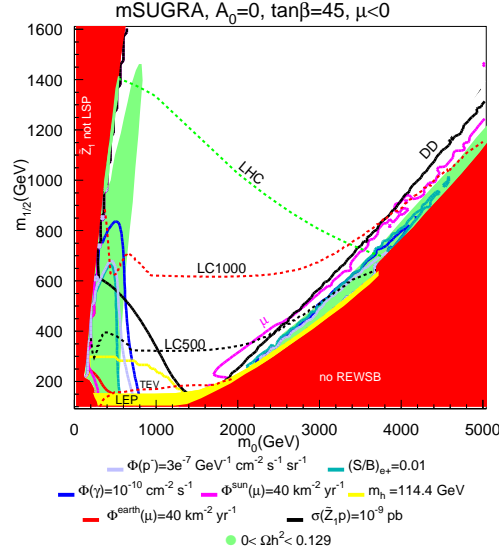


Fig. 4. The projected reach of various colliders, direct and indirect dark matter search experiments in the $mSUGRA$ model. For the indirect search results we have adopted the conservative default *DarkSUSY* isotropic DM halo density distribution. Plot is from Ref.⁸⁷

from other energy depositions such as charged pions, or hard photons where in addition a charged track is nearby. In this case, a SUSY search may still be made by looking for multi-jet plus *multi-muon* production, again without any requirement on missing E_T .⁴² Atlas and CMS are already reliably detecting cosmic muons. Also, muons enjoy an advantage over electrons in that they can be detected reliably to p_T values as low as 5 GeV.

The multiplicity of muons in ≥ 4 jet events is shown in Fig. 5, assuming $p_T(\mu) > 10$ GeV to remove BG from heavy flavor decays in SM processes. Here, we see that as one moves to high muon multiplicity, the SM background drops off sharply, and by $n_\mu \geq 3$, signal already far exceeds BG, at least for the SPS1a' signal point shown in the figure. In fact, by requiring *same-sign dimuon* plus multi-jet events, already signal in many cases will exceed background. The LHC should be able to discover gluinos with $m_{\tilde{g}} \sim 450$ (550) GeV in the SS dimuon plus ≥ 4 jets state with just 0.04 (0.1) fb^{-1} of integrated luminosity.

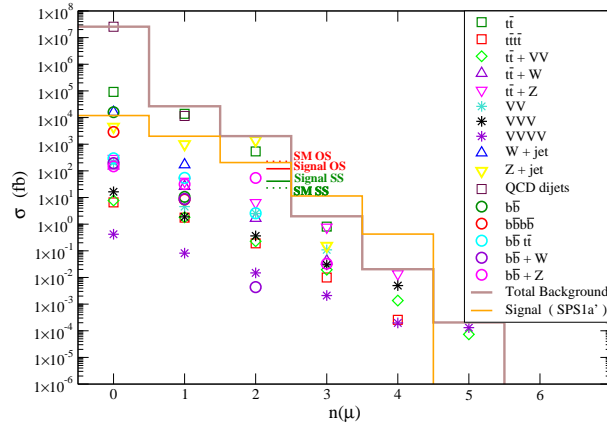


Fig. 5. Multiplicity of isolated muons in ≥ 4 jets events, from signal point $SPS1a'$ and various SM background processes.

4.4. Determination of particle properties

Once a putative signal for new physics emerges at LHC, the next step is to establish its origin. This will entail detailed measurements of cross sections and distributions in various event topologies to gain insight into the identity of the new particles being produced, their masses, decay patterns, spins, couplings (gauge quantum numbers) and ultimately mixing angles. These measurements are not straightforward in the LHC environment because of numerous possible SUSY production reactions occurring simultaneously, a plethora of particle cascade decay possibilities, hadronic debris from initial state radiation and lack of invariant mass reconstruction due to the presence of \cancel{E}_T . All these lead to ambiguities and combinatoric problems in reconstructing exactly what sort of signal reactions are taking place. In contrast, at the ILC, the initial state is simple, the beam energy is tunable and beam polarization can be used to select out specific processes.

While it seems clear that the ILC is better suited for a systematic program of precision particle measurements, studies have shown (albeit in special cases) that interesting measurements are also possible at the LHC. We go into just a subset of all details here in order to give the reader an idea of some of the possibilities suggested in the literature.

One suggested starting point is the distribution of effective mass $M_{\text{eff}} = \cancel{E}_T + \sum E_T(\text{jets})$ in the inclusive SUSY sample, which sets the approximate mass scale $M_{\text{SUSY}} \equiv \min(m_{\tilde{g}}, m_{\tilde{q}})$ for the strongly interacting particles are being produced,⁴³ and provides a measure of M_{SUSY} to 10-15%.

More detailed information on sparticle masses may be accessed by studying specific event topologies. For instance, the mass of dileptons from $\tilde{Z}_2 \rightarrow \ell^+ \ell^- \tilde{Z}_1$ decays is bounded by $m_{\tilde{Z}_2} - m_{\tilde{Z}_1}$ (this bound is even more restrictive if \tilde{Z}_2 decays via an on-shell slepton).⁴⁴ We therefore expect an OSSF invariant mass distribution to exhibit an edge at $m_{\tilde{Z}_2} - m_{\tilde{Z}_1}$ (or below) in any sample of SUSY events so long as the “spoiler” decay modes $\tilde{Z}_2 \rightarrow \tilde{Z}_1 Z$ or $\tilde{Z}_1 h$ are closed. Contamination from chargino production can be statistically removed by subtracting out the distribution of OSDF dileptons. In MHDM models, there may be more than one visible mass edge because the \tilde{Z}_3 may also be accessible in cascade decays.

In the happy circumstance where production of gluinos or a single type of squark is dominant, followed by a string of two-body decays, then further invariant mass edges are possible. One well-studied example comes from $\tilde{g} \rightarrow b\bar{b}_1 \rightarrow b\bar{b}\tilde{Z}_2 \rightarrow b\bar{b}\ell\bar{\ell}\tilde{Z}_1$; then one can try to combine a b -jet with the dilepton pair to reconstruct the squark-neutralino mass edge: $m(b\bar{\ell}\bar{\ell}) < m_{\tilde{b}_1} - m_{\tilde{Z}_1}$. Next, combining with another b -jet can yield a gluino-neutralino edge: $m(b\bar{b}\bar{\ell}\bar{\ell}) < m_{\tilde{g}} - m_{\tilde{Z}_1}$. The reconstruction of such a decay chain may be possible as shown in Ref.,⁴³ where other sequences of two-body decays are also examined. In practice, such fortuitous circumstances may not exist, and there are many combinatoric issues to overcome as well. A different study⁴⁵ shows that end-point measurements at the LHC will make it possible to access the mass difference between the LSP and the stau in a mSUGRA scenario where the stau co-annihilation mechanism is operative.

These end-point measurements generally give mass differences, not masses. However, by an analysis of the decay chain $\tilde{q}_L \rightarrow q\tilde{Z}_2 \rightarrow q\bar{\ell}^\pm\ell^\mp \rightarrow q\bar{\ell}^\pm\ell^\mp\tilde{Z}_1$, it has been argued⁴⁶ that reconstruction of masses may be possible under fortuitous circumstances. More recently, it has been suggested that it may be possible to directly access the gluino and/or squark masses (not mass differences) via the introduction of the so-called m_{T2} variable. We will refer the reader to the literature for details.⁴⁷ It also may be possible to make a measurement of $m_{\tilde{g}}$ based on total production cross section in cases where pure gluino pair production is dominant.⁴⁸

Mass measurements allow us to check consistency of specific SUSY models with a handful of parameters, and together with other measurements can readily exclude such models. But these are not the only interesting measurements at the LHC. It has been shown that if the NLSP of GMSB models decays into a superlight gravitino, it may be possible to determine its lifetime, and hence the gravitino mass at the LHC.⁴⁹ This will then allow one to infer the underlying SUSY breaking scale, a scale at least as

important as the weak scale! A recent study⁵⁰ suggests that this is possible even when the the decay length of the NLSP is too short to be measured. While linear collider experiments will ultimately allow the precision measurements that will directly determine the new physics to be softly broken supersymmetry,⁵¹ it will be exciting to analyze real LHC data that will soon be available to unravel many of the specific details about how (or if) SUSY is actually implemented in nature.

4.5. *Measuring DM properties at LHC and ILC*

SUSY discovery will undoubtedly be followed by a program (as outlined in Sec. 4.4) to reconstruct sparticle properties. What will we be able to say about dark matter in light of these measurements? Such a study was made by Baltz *et al.*⁵² where four mSUGRA case study points (one each in the bulk region, the HB/FP region, the stau coannihilation region and the A -funnel region) were examined for the precision with which measurements of sparticle properties that could be made at LHC, and also at a $\sqrt{s} = 0.5$ and 1 TeV e^+e^- collider. They then adopted a 24-parameter version of the MSSM and fit its parameters to these projected measurements. The model was then used to predict several quantities relevant to astrophysics and cosmology: the dark matter relic density $\Omega_{\tilde{Z}_1} h^2$, the spin-independent neutralino-nucleon scattering cross section $\sigma_{SI}(\tilde{Z}_1 p)$, and the neutralino annihilation cross section times relative velocity, in the limit that $v \rightarrow 0$: $\langle \sigma v \rangle|_{v \rightarrow 0}$. The last quantity is the crucial particle physics input for estimating signal strength from neutralino annihilation to anti-matter or gammas in the galactic halo. What this yields then is a *collider measurement* of these key dark matter quantities.

As an illustration, we show in Fig. 6 (taken from Ref.⁵²) the precision with which the neutralino relic density is constrained by collider measurements for the LCC2 point which is in the HB/FP region of the mSUGRA model. Measurements at the LHC cannot fix the LSP composition, and so are unable to resolve the degeneracy between a wino-LSP solution (which gives a tiny relic density) and the true solution with MHDm. Determinations of chargino production cross sections at the ILC can easily resolve the difference. It is nonetheless striking that up to this degeneracy ambiguity, experiments at the LHC can pin down the relic density to within $\sim 50\%$ (a remarkable result, given that there are sensible models where the predicted relic density may differ by orders of magnitude!). This improves to 10-20% if we can combine LHC and ILC measurements.

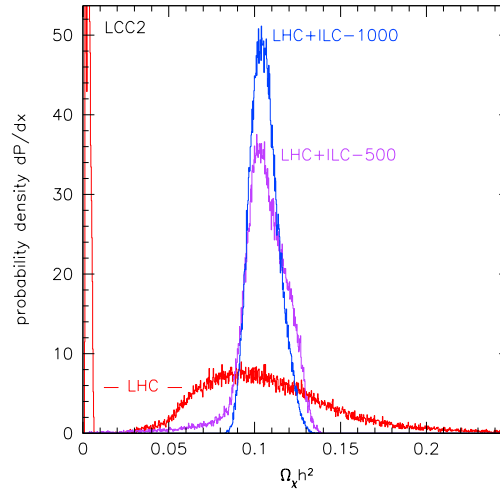


Fig. 6. Determination of neutralino relic abundance via measurements at the LHC and ILC, taken from Ref.⁵²

This collider determination of the relic density is very important. If it agrees with the cosmological measurement it would establish that the DM is dominantly thermal neutralinos from the Big Bang. If the neutralino relic density from colliders falls significantly below (1), it would provide direct evidence for multi-component DM— perhaps neutralinos plus axions or other exotica. Alternatively, if the collider determination gives a much larger value of $\Omega_{\tilde{Z}_1} h^2$, it could point to a long-lived but unstable neutralino and/or non-thermal DM.

The collider determination of model parameters would also pin down the neutralino-nucleon scattering cross section. Then if a WIMP signal is actually observed in DD experiments, one might be able to determine the local DM density of neutralinos and aspects of their velocity distribution based on the DD signal rate. This density should agree with that obtained from astrophysics if the DM in our Galaxy is comprised only of neutralinos.

Finally, a collider determination of $\langle\sigma v\rangle|_{v\rightarrow 0}$ would eliminate uncertainty on the particle physics side of projections for any ID signal from annihilation of neutralinos in the galactic halo. Thus, the observation of a gamma ray and/or anti-matter signal from neutralino halo annihilations would facilitate the determination of the galactic halo dark matter density distribution.

4.6. *Some non-SUSY WIMPs at the LHC*

4.6.1. B_μ^1 state from universal extra dimensions

Models with Universal Extra Dimensions, or UED, are interesting constructs which provide a foil for SUSY search analyses.⁵³ In the 5-D UED theory, one posits that the fields of the SM actually live in a 5-D brane world. The extra dimension is “universal” since *all* the SM particles propagate in the 5-D bulk. The single extra dimension is assumed to be compactified on a S_1/Z_2 orbifold (line segment). After compactification, the 4-D effective theory includes the usual SM particles, together with an infinite tower of Kaluza-Klein (KK) excitations. The masses of the excitations depend on the radius of the compactified dimension, and the first ($n = 1$) KK excitations can be taken to be of order the weak scale. In these theories, KK-parity $(-1)^n$ can be a conserved quantum number. If this so-called KK-parity is exact, then the lightest odd KK parity state will be stable and can be a DM candidate. At tree-level, all the KK excitations in a given level are essentially degenerate. Radiative corrections break the degeneracy, leaving colored excitations as the heaviest excited states and the $n = 1$ KK excitation of the SM $U(1)_Y$ gauge boson B_μ^1 as the lightest⁵⁴ KK odd state: in the UED case, therefore, the DM particle has spin-1. The splitting caused by the radiative corrections is also essential to assess how the KK excitations decay, and hence are crucial for collider phenomenology.⁵⁵

The relic density of B_μ^1 particles has been computed, and found to be compatible with observation for certain mass ranges of B_μ^1 .⁵⁶ Also, in UED, the colored excitations can be produced with large cross sections at the LHC, and decay via a cascade to the B_μ^1 final state. Thus, the collider signatures are somewhat reminiscent of SUSY, and it is interesting to ask whether it is possible to distinguish a *jets+leptons*+ \cancel{E}_T signal in UED from that in SUSY. Several studies⁵⁷ answer affirmatively, and in fact provide strong motivation for the measurement of the spins of the produced new particles.⁵⁸ UED DM generally leads to a large rate in IceCube, and may also give an observable signal in anti-protons and possibly also in photons and positrons.^{53,59} DD is also possible but the SI cross section is typically smaller than 10^{-9} pb.

4.6.2. *Little Higgs models*

Little Higgs models^{60,61} provide an alternative method compared to SUSY to evade the quadratic sensitivity of the scalar Higgs sector to ultra-violet (UV) physics. In this framework, the Higgs boson is a pseudo-Goldstone

boson of a spontaneously broken global symmetry that is not completely broken by any one coupling, but is broken when *all* couplings are included. This then implies that there is quadratic sensitivity to UV physics, but only at the multi-loop level. Specific models where the quadratic sensitivity enters at the two-loop level should, therefore, be regarded as low energy effective theories valid up to a scale $\Lambda \sim 10$ TeV, at which a currently unknown, and perhaps strongly-coupled UV completion of the theory is assumed to exist. Models that realize this idea require new TeV-scale degrees of freedom that can be searched for at the LHC: new gauge bosons, a heavy top-like quark, and new spin-zero particles, all with couplings to the SM. These models, however, run into phenomenological difficulties with precision EW constraints, unless a discrete symmetry—dubbed T -parity⁶²—is included. SM particles are then T -even, while the new particles are T -odd.

We will set aside the issue of whether T -parity conservation is violated by anomalies,⁶⁴ and assume that a conserved T -parity can be introduced.⁶⁵ In this case, the lightest T -odd particle A_H – the Little Higgs partner of the hypercharge gauge boson with a small admixture of the neutral W_{3H} boson – is stable and yields the observed amount of DM for a reasonable range of model parameters.⁵⁹ In this case, the DM particle has spin-1, though other cases with either a spin- $\frac{1}{2}$ or spin-0 heavy particle may also be possible. A_H can either annihilate with itself into vector boson pairs or $t\bar{t}$ pairs via s -channel Higgs exchange, or into top pairs via exchange of the heavy T -odd quark in the t -channel. Co-annihilation may also be possible if the heavy quark and A_H are sufficiently close in mass. Signals at the LHC^{66,67} mainly come from pair production of heavy quarks $pp \rightarrow T\bar{T}X$ followed by $T \rightarrow tA_H$ decay, and from single production of the heavy quark in association with A_H . These lead to $t\bar{t} + \cancel{E}_T$ events at LHC.⁶⁸ The \cancel{E}_T comes from the escaping A_H particle, which must be the endpoint of all T -odd particle decays.^a If A_H is the dominant component of galactic DM, we will generally expect small DD and ID rates for much the same reasons that the signals from the bino LSP tend to be small:⁵⁹ see, however, Ref.⁷⁰ for a different model with large direct detection rate.

^aWe note here that it is also possible to construct so-called twin-Higgs models⁶⁹ where the Higgs sector is stabilized via new particles that couple to the SM Higgs doublet, but are singlets under the SM gauge group. In this case, there would be no obvious new physics signals at the LHC.

5. Lecture 4: \cancel{E}_T and the dark matter connection

5.1. Neutralino relic density

Once a SUSY model is specified, then given a set of input parameters, it is possible to compute all superpartner masses and couplings necessary for phenomenology. We can then use these to calculate scattering cross sections and sparticle decay patterns to evaluate SUSY signals (and corresponding SM backgrounds) in collider experiments. We can also check whether the model is allowed or excluded by experimental constraints, either from direct SUSY searches, *e.g.* at LEP2 which requires that $m_{\tilde{W}_1} > 103.5$ GeV, $m_{\tilde{e}} \gtrsim 100$ GeV, and $m_h > 114.4$ GeV (for a SM-like light SUSY Higgs boson h), or from indirect searches through loop effects from SUSY particles in low energy measurements such as $B(b \rightarrow s\gamma)$ or $(g-2)_\mu$. We can also calculate the expected thermal LSP relic density. To begin our discussion, we will first assume that the lightest neutralino \tilde{Z}_1 is the candidate DM particle.

As mentioned earlier, the relic density calculation involves solving the Boltzmann equation, where the neutralino density changes due to both the expansion of the Universe and because of neutralino annihilation into SM particles, determined by the thermally averaged $\tilde{Z}_1\tilde{Z}_1$ annihilation cross section. An added complication occurs if neutralino *co-annihilation* is possible. Co-annihilation occurs if there is another SUSY particle close in mass to the \tilde{Z}_1 , whose thermal relic density (usually suppressed by the Boltzmann factor $\exp(-\frac{\Delta M}{T})$) is also significant. In the mSUGRA model, co-annihilation may occur from a stau, $\tilde{\tau}_1$, a stop \tilde{t}_1 or the lighter chargino \tilde{W}_1 . For instance, in some mSUGRA parameter-space regions the $\tilde{\tau}_1$ and \tilde{Z}_1 are almost degenerate, so that they both have a significant density in the early universe, and reactions such as $\tilde{Z}_1\tilde{\tau}_1 \rightarrow \tau\gamma$ occur. Since the electrically charged $\tilde{\tau}_1$ can also annihilate efficiently via electromagnetic interactions, this process also alters the equilibrium density of neutralinos. All in all, there are well over a thousand neutralino annihilation and co-annihilation reactions that need to be computed, involving of order 7000 Feynman diagrams. There exist several publicly available computer codes that compute the neutralino relic density: these include DarkSUSY,⁷¹ MicroMegas⁷² and IsaReD⁷³ (a part of the Isatools package of Isajet²⁸).

As an example, we show in Fig. 7 the m_0 vs. $m_{1/2}$ plane from the mSUGRA model, where we take $A_0 = 0$, $\mu > 0$, $m_t = 171.4$ GeV and $\tan\beta = 10$. The red-shaded regions are not allowed because either the $\tilde{\tau}_1$ becomes the lightest SUSY particle, in contradiction to negative searches for long lived, charged relics (left edge), or EWSB is not correctly obtained

(lower-right region). The blue-shaded region is excluded by LEP2 searches for chargino pair production ($m_{\tilde{W}_1} < 103.5$ GeV). We show contours of squark (solid) and gluino (dashed) mass (which are nearly invariant under change of A_0 and $\tan\beta$). Below the magenta contour near $m_{1/2} \sim 200$ GeV, $m_h < 110$ GeV, which is roughly the LEP2 lower limit on m_h in the model. The thin green regions at the edge of the unshaded white region has $0.094 < \Omega_{\tilde{Z}_1} h^2 < 0.129$ where the neutralino saturates the observed relic density. In the adjoining yellow regions, $\Omega_{\tilde{Z}_1} h^2 < 0.094$, so these regions require multiple DM components. The white regions all have $\Omega_{\tilde{Z}_1} h^2 > 0.129$ and so give too much thermal DM: they are excluded in the standard Big Bang cosmology.

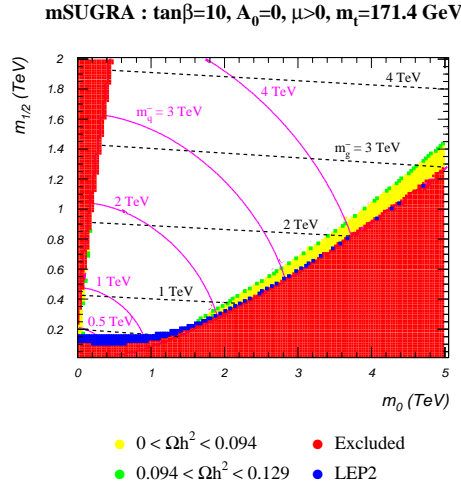


Fig. 7. DM-allowed regions in the $m_0 - m_{1/2}$ plane of the mSUGRA model for $\tan\beta = 10$ with $A_0 = 0$ and $\mu > 0$.

The DM-allowed regions are classified as follows:

- At very low m_0 and low $m_{1/2}$ values is the so-called *bulk* annihilation region.⁷⁴ Here, sleptons are quite light, so $\tilde{Z}_1 \tilde{Z}_1 \rightarrow \ell \bar{\ell}$ via t -channel slepton exchange. In years past (when $\Omega_{\text{CDM}} h^2 \sim 0.3$ was quite consistent with data), this was regarded as the favored region. But today LEP2 sparticle search limits have increased the LEP2-forbidden region

from below, while the stringent bound $\Omega_{CDM}h^2 \leq 0.13$ has pushed the DM-allowed region down. Now hardly any bulk region survives in the mSUGRA model.

- At low m_0 and moderate $m_{1/2}$, there is a thin strip of (barely discernable) allowed region adjacent to the stau-LSP region where the neutralino and the lighter stau were in thermal equilibrium in the early universe. Here co-annihilation with the light stau serves to bring the neutralino relic density down to its observed value.⁷⁵
- At large m_0 , adjacent to the EWSB excluded region on the right, is the hyperbolic branch/focus point (HB/FP) region, where the superpotential μ parameter becomes small and the higgsino-content of \tilde{Z}_1 increases significantly. Then \tilde{Z}_1 can annihilate efficiently via gauge coupling to its higgsino component and becomes mixed higgsino-bino DM. If $m_{\tilde{Z}_1} > M_W, M_Z$, then $\tilde{Z}_1\tilde{Z}_1 \rightarrow WW, ZZ, Zh$ is enhanced, and one finds the correct measured relic density.⁷⁶

We show the corresponding situation for $\tan\beta = 52$ in Fig. 8. While the stau co-annihilation and the HB/FP regions are clearly visible, we see that a large DM consistent region now appears.

- In this region, the value of m_A is small enough so that $\tilde{Z}_1\tilde{Z}_1$ can annihilate into $b\bar{b}$ pairs through s -channel A (and also H) resonance. This region has been dubbed the A -funnel.⁷⁷ It can be very broad at large $\tan\beta$ because the width Γ_A can be quite wide due to the very large b - and τ - Yukawa couplings. If $\tan\beta$ is increased further, then $\tilde{Z}_1\tilde{Z}_1$ annihilation through the (virtual) A^* is large all over parameter space, and most of the theoretically-allowed parameter space becomes DM-consistent. For even higher $\tan\beta$ values, the parameter space collapses due to a lack of appropriate EWSB.

It is also possible at low $m_{1/2}$ values that a light Higgs h resonance annihilation region can occur just above the LEP2 excluded region.⁷⁸ Finally, if A_0 is large and negative, then the \tilde{t}_1 can become light, and $m_{\tilde{t}_1} \sim m_{\tilde{Z}_1}$, so that stop-neutralino co-annihilation⁷⁹ can occur.

Up to now, we have confined our discussion to the mSUGRA framework in which compatibility with (1) is obtained only over selected portions of the $m_0 - m_{1/2}$ plane. The reader may well wonder what happens if we relax the untested universality assumptions that underlie mSUGRA. Without going into details, we only mention here that in many simple one-parameter extensions of mSUGRA where the universality of mass parameters is relaxed in any one of the matter scalar, the Higgs scalar, or the gaugino sectors,

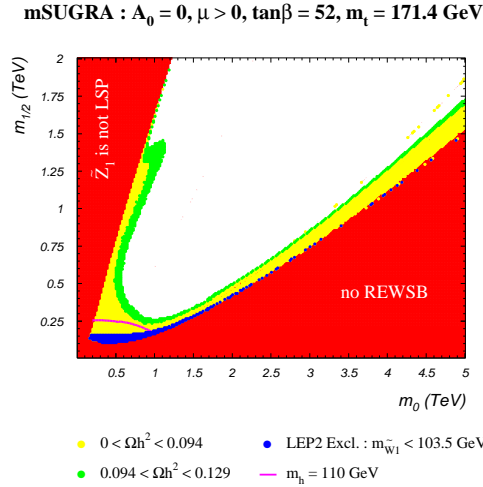


Fig. 8. *DM-allowed regions in the $m_0 - m_{1/2}$ plane of the mSUGRA model for $\tan\beta = 52$ with $A_0 = 0$ and $\mu > 0$. The various colors of shading is as in Fig. 7.*

all points in the $m_0 - m_{1/2}$ plane become compatible with the relic density constraint due to a variety of mechanisms: these are catalogued in Ref.⁸⁰ Implications of the relic density measurement for collider searches must thus be drawn with care.

5.2. Neutralino direct detection

Fits to galactic rotation curves imply a local relic density of $\rho_{CDM} \sim 0.3 \text{ GeV/cm}^3$. For a 100 GeV WIMP, this translates to about one WIMP per coffee mug volume at our location in the galaxy. The goal of DD experiments is to detect the very rare WIMP-nucleus collisions that should be occurring as the earth, together with the WIMP detector, moves through the DM halo.

DD experiments are usually located deep underground to shield the experimental apparatus from background due to cosmic rays and ambient radiation from the environment or from radioactivity induced by cosmic ray exposure. One technique is to use cryogenic crystals cooled to near absolute zero, and look for phonon and ionization signals from nuclei recoiling from a WIMP collision. In the case of the CDMS experiment⁸¹ at the Soudan iron mine, target materials include germanium and silicon. Another technique uses noble gases cooled to a liquid state as the target. Here, the signal is

scintillation light picked up by photomultiplier tubes and ionization. Target materials include xenon,⁸² argon and perhaps neon. These noble liquid detectors can be scaled up to large volumes at relatively low cost. They have the advantage of fiducialization, wherein the outer layers of the detector act as an active veto against cosmic rays or neutrons coming from phototubes or detector walls: only single scatters from the inner fiducial volume qualify as signal events. A third technique, typified by the COUPP experiment,⁸³ involves use of superheated liquids such as CF^3I located in a transparent vessel. The nuclear recoil from a WIMP-nucleon collision then serves as a nucleation site, so that a bubble forms. The vessel is monitored visually by cameras. Background events are typically located close to the vessel wall, while neutron interactions are likely to cause several bubbles to form, instead of just one, as in a WIMP collision. This technique allows for the use of various target liquids, including those containing elements such as fluorine, which is sensitive to *spin-dependent* interactions.

The cross section for WIMP-nucleon collisions can be calculated, and in the low velocity limit separates into a coherent spin-independent component (from scattering mediated by scalar quarks and scalar Higgs bosons) which scales as nuclear mass squared, and a spin-dependent component from scattering mediated by the Z boson or by squarks, which depends on the WIMP and nuclear spins.⁹ The scattering cross section per nucleon versus m_{WIMP} serves as a figure of merit and facilitates the comparison of the sensitivity of various experiments using different target materials.

In Fig. 9, we show the spin-independent $\tilde{Z}_1 p$ cross section versus $m_{\tilde{Z}_1}$ for a large number of SUSY models (including mSUGRA). Every color represents a different model. For each model, parameters are chosen so that current collider constraints on sparticle masses are satisfied, and further, that the lightest neutralino (assumed to be the LSP) saturates the observed relic abundance of CDM. Also shown is the sensitivity of current experiments together with projected sensitivity of proposed searches at superCDMS, Xenon-100, LUX, WARP and at a ton-sized noble liquid detector. The details of the various models are unimportant for our present purpose. The key thing to note is that while the various models have a branch where $\sigma_{SI}(p\tilde{Z}_1)$ falls off with $m_{\tilde{Z}_1}$, there is another branch where this cross-section asymptotes to just under 10^{-8} pb.^{80,84,85} Points in this-branch (which includes the HB/FP region of mSUGRA), are consistent with (1) because \tilde{Z}_1 has a significant higgsino component. Neutralinos with an enhanced higgsino content can annihilate efficiently in the early universe via gauge interactions. Moreover, since the spin-independent DD ampli-

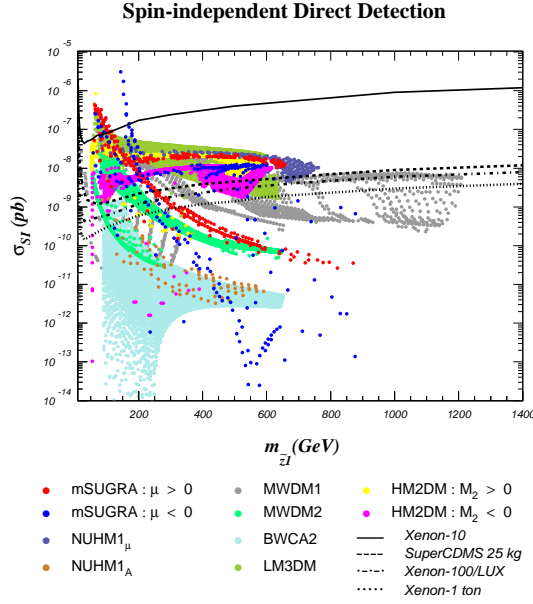


Fig. 9. The spin-independent neutralino-proton scattering cross-section vs $m_{\tilde{Z}_1}$ in a variety of SUSY models, compatible with collider constraints where thermally produced Big Bang neutralinos saturate the observed dark matter density.

tude is mostly determined by the Higgs boson-higgsino-gaugino coupling, it is large in models with MHDM which has both gaugino and higgsino components. Thus the enhanced higgsino component of MHDM increases both the neutralino annihilation in the early universe as well as the spin-independent DD rate. The exciting thing is that the experiments currently being deployed— such as Xenon-100, LUX and WARP— will have the sensitivity to probe this class of models. To go further will require ton-size or greater target material.

We note here that if $m_{\text{WIMP}} \lesssim 150$ GeV, then it may be possible to extract the WIMP mass by measuring the energy spectrum of the recoiling nuclear targets.⁸⁶ Typically, of order 100 or more events are needed for such a determination to 10-20%. For higher WIMP masses, the recoil energy spectrum varies little, and WIMP mass extraction is much more difficult. Since the energy transfer from the WIMP to a nucleus is maximized when the two have the same mass, DD experiments with several target nuclei

ranging over a wide range of masses would facilitate the distinction between somewhat light and relatively heavy WIMPs, and so, potentially serve to establish the existence of multiple WIMP components in our halo.

5.3. *Indirect detection of neutralinos*

There are also a number of indirect WIMP search techniques that attempt to detect the decay products from WIMP annihilation at either the center of the sun, at the galactic center, or within the galactic halo.

5.3.1. *Neutrino telescopes*

Neutrino telescopes such as ANTARES or IceCube can search for high energy neutrinos produced from WIMP-WIMP annihilation into SM particles in the core of the sun (or possibly the earth). The technique involves detection of multi-tens of GeV muons produced by ν_μ interactions with polar ice (IceCube) or ocean water (ANTARES). The muons travel at speeds greater than the speed of light in the medium, thus leaving a tell-tale signal of Cerenkov light which is picked up by arrays of phototubes. The IceCube experiment, currently being deployed at the south pole, will monitor a cubic kilometer of ice in search of $\nu_\mu \rightarrow \mu$ conversions. It should be fully deployed by 2011. The experiment is mainly sensitive to muons with $E_\mu > 50$ GeV.

In the case of neutralinos of SUSY, mixed higgsino dark matter (MHDM) has a large (spin-dependent) cross-section to scatter from hydrogen nuclei via Z -exchange and so is readily captured. Thus, in the HB/FP region of mSUGRA, or in other SUSY models with MHDM, we expect observable levels of signal exceeding 40 events/km²/yr with $E_\mu > 50$ GeV. For the mSUGRA model, the IceCube signal region is shown beneath the magenta contour labelled μ in Fig. 4.⁸⁷ These results were obtained using the Isajet-DarkSUSY interface.⁷¹ Notice that DD signals are also observable in much the same region (below the contour labelled DD) where the neutralino is MHDM.

5.3.2. *Anti-matter from WIMP halo annihilations*

WIMP annihilation in the galactic halo offers a different possibility for indirect DM searches. Halo WIMPs annihilate equally to matter and anti-matter, so the rare presence of high energy anti-matter in cosmic ray events – positrons e^+ , anti-protons \bar{p} , or even anti-deuterons \bar{D} – offer possible signatures. Positrons produced in WIMP annihilations must originate relatively close by, or else they will find cosmic electrons to annihilate against,

or lose energy via bremsstrahlung. Anti-protons and anti-deuterons could originate further from us because, being heavier, they are deflected less and so lose much less energy. The expected signal rate depends on the WIMP annihilation rate into anti-matter, the model for the propagation of the anti-matter from its point of origin to the earth, and finally on the assumed profile of the dark matter in the galactic halo. Several possible halo density profiles are shown in Fig. 10. We see that while the *local* WIMP density is inferred to a factor of ~ 2 -3 (we are at about 8 kpc from the Galactic center), the DM density at the galactic center is highly model-dependent close to the core. Since the ID signal should scale as the square of the WIMP density at the source, positron signals will be uncertain by a factor of a few with somewhat larger uncertainty for \bar{p} and \bar{D} signals that originate further away. Anti-particle propagation through the not so well known magnetic field leads to an additional uncertainty in the predictions. The recently launched Pamela space-based anti-matter telescope can look for e^+ or \bar{p} events while the balloon-borne GAPS experiment will be designed to search for anti-deuterons. Anti-matter signals tend to be largest in the case of SUSY models with MHDM or when neutralinos annihilate through the A -resonance.⁸⁸

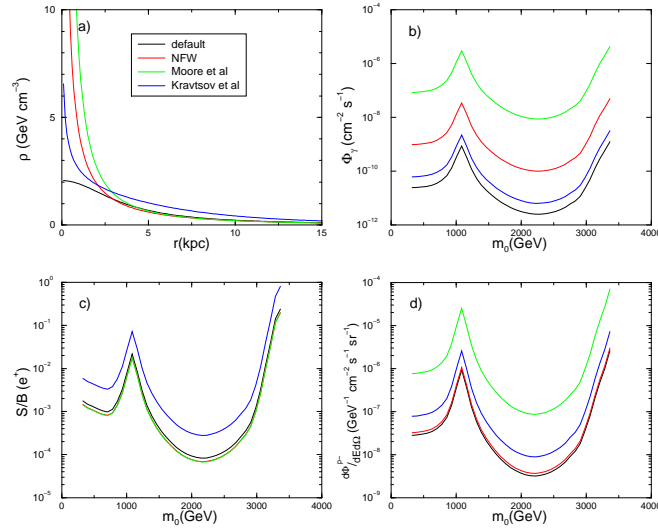


Fig. 10. Various predictions for the DM halo in the Milky Way as a function of distance from the galactic center. The earth is located at $r \sim 8$ kpc.

5.3.3. *Gamma rays from WIMP halo annihilations*

As mentioned in the Introduction, high energy gamma rays from WIMP annihilation offer some advantages over the signal from charged antiparticles. Gamma rays would point to the source, and would degrade much less in energy during their journey to us. This offers the possibility of the line signal from $\tilde{Z}_1\tilde{Z}_1 \rightarrow \gamma\gamma$ processes that occur via box and triangle diagrams. While this reaction is loop-suppressed, it yields monoenergetic photons with $E_\gamma \simeq m_{\text{WIMP}}$, and so can provide a measure of the WIMP mass. Another possibility is to look for continuum gamma rays from WIMP annihilation to hadrons where, for instance, the gamma is the result of π^0 decays. Since the halo WIMPs are essentially at rest, we expect a diffuse spectrum of gamma rays, but with $E_\gamma < m_{\text{WIMP}}$. Because gamma rays can traverse large distances, a good place to look at is the galactic center, where the WIMP density (see Fig. 10) is expected to be very high. Unfortunately, the density at the core is also very uncertain, making predictions for the gamma ray flux uncertain by as much as four orders of magnitude. Indeed, detection of WIMP halo signals may serve to provide information about the DM distribution in our galaxy.

Anomalies have been reported in the cosmic gamma ray spectrum. In one example, the Egret experiment⁸⁹ sees an excess of gamma rays with $E_\gamma > 1$ GeV. Explanations for the Egret GeV anomaly range from $\tilde{Z}_1\tilde{Z}_1 \rightarrow b\bar{b} \rightarrow \gamma$ with $m_{\tilde{Z}_1} \sim 60$ GeV,⁹⁰ to mis-calibration of the Egret calorimeter.⁹¹ The GLAST gamma ray observatory is scheduled for lift-off in 2008 and should help resolve this issue, as will the upcoming LHC searches.⁹²

5.4. *Gravitino dark matter*

In gravity-mediated SUSY breaking models, gravitinos typically have weak scale masses and, because they only have tiny gravitational couplings, are usually assumed to be irrelevant for particle physics phenomenology. Cosmological considerations, however, lead to the *gravitino problem*, wherein overproduction of gravitinos, followed by their late decays into SM particles, can disrupt the successful predictions of Big Bang nucleosynthesis. The gravitino problem can be overcome by choosing an appropriate range for $m_{\tilde{G}}$ and a low enough re-heat temperature for the universe after inflation⁹³ as illustrated in Fig. 11, or by hypothesizing that the \tilde{G} is in fact the stable LSP, and thus constitutes the DM.⁹⁴

Here, we consider the consequences of a gravitino LSP in SUGRA models. If gravitinos are produced in the pre-inflation epoch, then their number

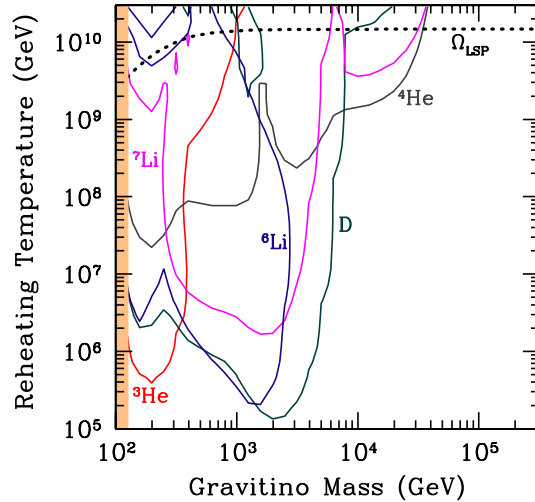


Fig. 11. An illustration of constraints from Big Bang nucleosynthesis which require T_R to be below the various curves, for the HB/FP region of the $mSUGRA$ model with $m_0 = 2397$ GeV, $m_{1/2} = 300$ GeV, $A_0 = 0$ and $\tan\beta = 30$, from Kohri et al.⁹³ to which we refer the reader for more details.

density will be diluted away during inflation. After the universe inflates, it enters a re-heating period wherein all particles can be thermally produced. However, the couplings of the gravitino are so weak that though gravitinos can be produced by the particles that do partake of thermal equilibrium, gravitinos themselves never attain thermal equilibrium: indeed their density is so low that gravitino annihilation processes can be neglected in the calculation of their relic density. The thermal production (TP) of gravitinos in the early universe has been calculated, and including EW contributions, is given by the approximate expression (valid for $m_{\tilde{G}} \ll M_i$ ⁹⁵):

$$\Omega_{\tilde{G}}^{TP} h^2 \simeq 0.32 \left(\frac{10 \text{ GeV}}{m_{\tilde{G}}} \right) \left(\frac{m_{1/2}}{1 \text{ TeV}} \right)^2 \left(\frac{T_R}{10^8 \text{ GeV}} \right) \quad (13)$$

where T_R is the re-heat temperature.

Gravitinos can also be produced by decay of the next-to-lightest SUSY particle, the NLSP. In the case of a long-lived neutralino NLSP, the neutralinos will be produced as usual with a thermal relic abundance in the early universe. Later, they will each decay as $\tilde{Z}_1 \rightarrow \gamma\tilde{G}$, $Z\tilde{G}$ or $h\tilde{G}$. The total relic abundance is then

$$\Omega_{\tilde{G}} h^2 = \Omega_{\tilde{G}}^{TP} h^2 + \frac{m_{\tilde{G}}}{m_{\tilde{Z}_1}} \Omega_{\tilde{Z}_1} h^2. \quad (14)$$

The \tilde{G} from NLSP decay may constitute warm/hot dark matter depending in the $\tilde{Z}_1 - \tilde{G}$ mass gap, while the thermally produced \tilde{G} will be CDM.⁹⁶

The lifetime for neutralino decay to the photon and a gravitino is given by,⁹⁷

$$\begin{aligned} \tau(\tilde{Z}_1 \rightarrow \gamma\tilde{G}) &\simeq \frac{48\pi M_P^2}{m_{\tilde{Z}_1}^3} A^2 \frac{r^2}{(1-r^2)^3(1+3r^2)} \\ &\sim 5.8 \times 10^8 \text{ s} \left(\frac{100 \text{ GeV}}{m_{\tilde{Z}_1}} \right)^3 \frac{1}{A^2} \frac{r^2}{(1-r^2)^3(1+3r^2)}, \end{aligned}$$

where $A = (v_4^{(1)} \cos \theta_W + v_3^{(1)} \sin \theta_W)^{-1}$, with $v_{3,4}^{(1)}$ being the wino and bino components of the \tilde{Z}_1 ,⁸ M_P is the reduced Planck mass, and $r = m_{\tilde{G}}/m_{\tilde{Z}_1}$. Similar formulae (with different mixing angle and r -dependence) hold for decays to the gravitino plus a Z or h boson. We see that – except when the gravitino is very much lighter than the neutralino as may be the case in GMSB models with a low SUSY breaking scale – the NLSP decays well after Big Bang nucleosynthesis. Such decays would inject high energy gammas and/or hadrons into the cosmic soup post-nucleosynthesis, which could break up the nuclei, thus conflicting with the successful BBN predictions of Big Bang cosmology. For this reason, gravitino LSP scenarios usually favor a stau NLSP, since the BBN constraints in this case are much weaker.

Finally, we remark here upon the interesting interplay of baryogenesis via leptogenesis with the nature of the LSP and NLSP. For successful thermal leptogenesis to take place, it is found that the reheat temperature of the universe must exceed $\sim 10^{10}$ GeV.⁹⁸ If this is so, then gravitinos would be produced thermally with a huge abundance, and then decay late, destroying BBN predictions. For this reason, some adherents of leptogenesis tend to favor scenarios with a gravitino LSP, but with a stau NLSP.⁹⁹

5.5. Axion/axino dark matter

If we adopt the MSSM as the effective theory below M_{GUT} , and then seek to solve the strong CP problem via the Peccei-Quinn solution,¹⁰⁰ we must introduce not only an axion but also a spin- $\frac{1}{2}$ axino \tilde{a} into the theory. The axino mass is found to be in the range of keV-GeV,¹⁰¹ but its coupling is suppressed by the Peccei-Quinn breaking scale f_a , which is usually taken to be of order $10^9 - 10^{12}$ GeV: thus, the axino interacts more weakly than a WIMP, but not as weakly as a gravitino. Both the axion and axino can be compelling choices for DM in the universe.¹⁰²

Like the gravitino, the axino will likely not be in thermal equilibrium in the early universe, but can still be produced thermally via particle scattering. The thermal production abundance is given by^{102,103}

$$\Omega_{\tilde{a}}^{TP} h^2 \simeq 5.5 g_s^6 \log\left(\frac{1.108}{g_s}\right) \left(\frac{10^{11} \text{ GeV}}{f_a/N}\right)^2 \times \left(\frac{m_{\tilde{a}}}{100 \text{ MeV}}\right) \left(\frac{T_R}{10^4 \text{ GeV}}\right),$$

where f_a is the PQ scale, N is a model-dependent color anomaly factor that enters only as f_a/N , and g_s is the strong coupling at the reheating scale.

Also like the gravitino, the axino can be produced non-thermally by NLSP decays, where the NLSP abundance is given by the standard relic density calculation. Thus,

$$\Omega_{\tilde{a}} h^2 = \Omega_{\tilde{a}}^{TP} h^2 + \frac{m_{\tilde{a}}}{m_{NLSP}} \Omega_{NLSP} h^2. \quad (15)$$

In this case, the thermally produced axinos will be CDM for $m_{\tilde{a}} \gtrsim 0.1 \text{ MeV}$,¹⁰² while the axinos produced in NLSP decay will constitute hot/warm DM.⁹⁶ Since the PQ scale is considerably lower than the Planck scale, the lifetime for decays such as $\tilde{Z}_1 \rightarrow \gamma \tilde{a}$ are of order $\sim 0.01 - 1 \text{ sec}$ —well before BBN. Thus, the axino DM scenario is much less constrained than gravitino DM.

Note also that if axinos are the CDM of the universe, then models with very large $\Omega_{\tilde{Z}_1} h^2 \sim 100 - 1000$ can be readily accommodated, since there is a huge reduction in relic density upon \tilde{Z}_1 decay to the axino. This possibility occurs in models with multi-TeV scalars (and hence a multi-TeV gravitino) and a bino-like \tilde{Z}_1 . In this case— with very large $m_{\tilde{G}}$ — there is no gravitino problem as long as the re-heat temperature $T_R \sim 10^6 - 10^8 \text{ GeV}$. This range of T_R is also what is needed to obtain successful *non-thermal* leptogenesis (involving heavy neutrino N production via inflaton decay)¹⁰⁴ along with the correct abundance of axino dark matter.¹⁰⁸

5.5.1. Yukawa-unified SUSY with mixed axion/axino dark matter

The gauge group $SO(10)$ is very highly motivated in that it unifies all matter particles of each generation into a spinorial **16** dimensional representation. Included in the **16** is a state containing a SM gauge singlet right-hand neutrino. SUSY $SO(10)$ theories may also allow for third generation Yukawa coupling unification. In Ref.,^{105,106} it was found via scans over SUSY parameter space that in fact it is possible to find models with

Yukawa coupling unification, but only for certain choices of GUT scale SSB boundary conditions. Yukawa unified solutions can be found if

- $m_{16} \sim 3 - 15$ TeV,
- $m_{1/2}$ is very small,
- $\tan \beta \sim 50$,
- $A_0 \sim -2m_{16}$ with $m_{10} \sim 1.2m_{16}$,
- $m_{H_d} > m_{H_u}$ at M_{GUT} .

In this case, models with an inverted scalar mass hierarchy are found. The spectra is characterized by 1. first/second generation scalars in the 3-15 TeV range, 2. third generation scalars, m_A and μ in the few TeV range and 3. gluinos around 350-500 GeV, with charginos $\sim 100 - 160$ GeV and $\tilde{Z}_1 \sim 50 - 90$ GeV.

A problem emerges in that the calculated neutralino relic density is about $10^2 - 10^5$ times its measured value. A solution has been invoked that the axino and axion are instead the DM particles. In this case, neutralinos would still be produced at large rates in the early universe, but each neutralino would decay after a fraction of a second (slightly before the onset of BBN) to axino \tilde{a} plus photon. Then the relic axino density would be $(m_{\tilde{a}}/m_{\tilde{Z}_1})\Omega_{\tilde{Z}_1} h^2$, and the mass ratio out in front reduces the relic density by a factor of $10^{-2} - 10^{-5}$!. The neutralino is still long lived enough that it will give rise to missing energy at the LHC. In fact, since gluinos are so light, we would expect a gluino pair cross section of order 10^5 fb, along with decays $\tilde{g} \rightarrow b\tilde{b}\tilde{Z}_2$, $b\tilde{b}\tilde{Z}_1$ and $t\tilde{b}\tilde{W}_1 + c.c.$ ¹⁰⁷ These new physics reactions should be easily seen via isolated multi-muon plus jet production in the early stages of LHC running.

The Yukawa-unified SUSY scenario is also very appealing cosmologically. We would expect the gravitino mass to be of order m_{16} : 3-15 TeV. If it is heavier than about 5 TeV, then the gravitino decays with lifetime around 1 sec: right at the onset of BBN! This eliminates the BBN gravitino problem as long as re-heat temperature $T_R \lesssim 10^9$ GeV. Several scenarios of mixed axion/axino dark matter in Yukawa unified SUSY have been examined in Refs.^{108,109} It is found that one may accommodate either dominant axion or axino DM, but m_{16} at the high end. Values of $m_{16} \gtrsim 10$ TeV are preferred, as are high values for the PQ breaking scale: $f_a \gtrsim 10^{12}$ GeV. The values of T_R allowed can accommodate several baryogenesis mechanisms, for instance, non-thermal leptogenesis.

6. Conclusions

The union of particle physics, astrophysics and cosmology has reached an unprecedented stage. Today we are certain that the bulk of the matter in the universe is non-luminous, not made of any of the known particles, but instead made of one or more *new physics* particles that do not appear in the SM. And though we know just how much of this unknown dark matter there is, we have no idea *what* it is. Today, many theoretical speculations seek to answer one of the most pressing particle physics puzzles, “What is the origin of EWSB and how can we embed this into a unified theory of particle interactions?” The answer may automatically also point to a resolution of this 75 year old puzzle as to what the dominant matter component of our universe might be. Particle physicists have made many provocative suggestions for the origin of DM, including supersymmetry and extra spatial dimensions, ideas that will completely change the scientific paradigm if they prove to be right.

The exciting thing is that many of these speculations will be *directly tested* by a variety of particle physics experiments along with astrophysical and cosmological searches. The Large Hadron Collider, scheduled to commence operation in 2009, will directly study particle interactions at a scale of 1 TeV where new matter states are anticipated to exist for sound theoretical reasons. These new states may well be connected to the DM sector, and so in this way the LHC can make crucial contributions to not only particle physics, but also to cosmology. If indeed the LHC can make DM particles or their associated new physics states, then a large rate for signal events with jets, leptons and \cancel{E}_T is expected.

Any discovery at LHC of new particles at the TeV scale will make a compelling case for the construction of a lepton collider to study the properties of these particles in detail and to elucidate the underlying physics. Complementary to the LHC, there are a variety of searches for signals from relic dark matter particles either locally or dispersed throughout the galactic halo. The truly unprecedented thing about this program is that if our ideas connecting DM and the question of EWSB are correct, measurements of the properties of new particles produced at the LHC (possibly complemented by measurements at an electron-positron linear collider) may allow us to independently infer just how much DM there is in the universe, and quantitatively predict what other searches for DM should find.

7. Acknowledgments

I take this opportunity to thank Tao Han for organizing an exceptional TASI workshop, and K. T. Mahantappa for his hospitality and patience in organizing many TASI workshops.

8. References

References

1. D. N. Spergel *et al.* (WMAP Collaboration), *Astrophys. J. Supp.*, **170** (2007) 377.
2. Report of the DMSAG panel on http://www.science.doe.gov/hep/hepap_reports.shtml. See also, L. Roszkowski, *Pramana*, **62** (2004) 389.
3. For reviews, see *e.g.* C. Jungman, M. Kamionkowski and K. Griest, *Phys. Rept.* **267** (1996) 195; A. Lahanas, N. Mavromatos and D. Nanopoulos, *Int. J. Mod. Phys. D* **12** (2003) 1529; M. Drees, hep-ph/0410113; K. Olive, “Tasi Lectures on Astroparticle Physics”, astro-ph/0503065; G. Bertone, D. Hooper and J. Silk, *Phys. Rept.* **405** (2005) 279.
4. J. Feng and J. Kumar, arXiv:0803.4196 [hep-ph].
5. R. Kolb and M. Turner, *The Early Universe*, (Addison-Wesley, 1990).
6. J. Wess and B. Zumino, *Nucl. Phys. B* **70** (1974) 39.
7. A. Salam and J. Strathdee, *Nucl. Phys. B* **76** (1974) 477.
8. H. Baer and X. Tata, *Weak Scale Supersymmetry: From Superfields to Scattering Events*, (Cambridge University Press, 2006).
9. M. Drees, R. Godbole and P. Roy, *Sparticles*, (World Scientific, 2004).
10. P. Binétruy, *Supersymmetry* (Oxford, 2006).
11. S. Dimopoulos and H. Georgi, *Nucl. Phys. B* **193** (1981) 150.
12. B.C. Allanach, S. Kraml and W. Porod, *J. High Energy Phys.* **03** (2003) 016; G. Belanger, S. Kraml and A. Pukhov, *Phys. Rev. D* **72** (2005) 015003; S. Kraml and S. Sekmen in: *Physics at TeV Colliders 2007, BSM working group report*, in prep.; see <http://cern.ch/kraml/comparison>.
13. M. Dine, A. Nelson, Y. Nir and Y. Shirman, *Phys. Rev. D* **53** (1996) 2658; for a review, see G. Giudice and R. Rattazzi, *Phys. Rept.* **322** (1999) 419.
14. L. Randall and R. Sundrum, *Nucl. Phys. B* **557** (1999) 79; G. Giudice, M. Luty, H. Murayama and R. Rattazzi, *J. High Energy Phys.* **9812** (1998) 027.
15. S. Kachru, R. Kallosh, A. Linde and S. P. Trivedi, *Phys. Rev. D* **68** (2003) 046005; K. Choi, A. Falkowski, H. P. Nilles, M. Olechowski and S. Pokorski, *J. High Energy Phys.* **0411** (2004) 076; K. Choi, A. Falkowski, H. P. Nilles and M. Olechowski, *Nucl. Phys. B* **718** (2005) 113; K. Choi, K-S. Jeong and K. Okumura, *J. High Energy Phys.* **0509** (2005) 039; H. Baer, E. Park, X. Tata and T. Wang, *J. High Energy Phys.* **0706** (2007) 033, and references therein.
16. L. Everett, I.-W. Kim, P. Ouyang and K. Zurek, *Phys. Rev. Lett.* **101** (2008) 101803 and *J. High Energy Phys.* **0808** (2008) 102.
17. H. Baer and X. Tata, *Phys. Lett. B* **160** (1985) 159.
18. H. Baer, J. Ellis, G. Gelmini, D. V. Nanopoulos and X. Tata, *Phys. Lett.*

- B 161** (1985) 175; G. Gamberini, *Z. Physik C* **30** (1986) 605; H. Baer, V. Barger, D. Karatas and X. Tata, *Phys. Rev. D* **36** (1987) 96; H. Baer, X. Tata and J. Woodside, *Phys. Rev. D* **45** (1992) 142.
19. H. Baer, D. Dzialo-Karatas and X. Tata, *Phys. Rev. D* **42** (1990) 2259.
 20. H. Baer, C. H. Chen, F. Paige and X. Tata, *Phys. Rev. D* **50** (1994) 4508.
 21. H. Baer, C. H. Chen, F. Paige and X. Tata, *Phys. Rev. D* **49** (1994) 3283
 22. H. E. Haber and D. Wyler, *Nucl. Phys. B* **323** (1989) 267; S. Ambrosanio and B. Mele, *Phys. Rev. D* **53** (1996) 2541 and *Phys. Rev. D* **55** (1997) 1399 [Erratum-ibid. **D56**, 3157 (1997)]; H. Baer and T. Krupovnickas, *J. High Energy Phys.* **0209** (2002) 038.
 23. H. Baer and X. Tata, *Phys. Rev. D* **47** (1993) 2739.
 24. H. Baer, C. Chen, M. Drees, F. Paige and X. Tata, *Phys. Rev. Lett.* **79** (1997) 986.
 25. H. Baer, C. Chen, M. Drees, F. Paige and X. Tata, *Phys. Rev. D* **59** (1999) 015010.
 26. H. Baer, M. Bisset, X. Tata and J. Woodside, *Phys. Rev. D* **46** (1992) 303.
 27. H. Baer, M. Bisset, D. Dicus, C. Kao and X. Tata, *Phys. Rev. D* **47** (1993) 1062; H. Baer, M. Bisset, C. Kao and X. Tata, *Phys. Rev. D* **50** (1994) 316.
 28. ISAJET, by H. Baer, F. Paige, S. Protopopescu and X. Tata, hep-ph/0312045; see also H. Baer, J. Ferrandis, S. Kraml and W. Porod, *Phys. Rev. D* **73** (2006) 015010.
 29. M. Muhlleitner, A. Djouadi and Y. Mambrini, *Comput. Phys. Commun.* **168** (2005) 46.
 30. W. Porod, *Comput. Phys. Commun.* **153** (2003) 275.
 31. T. Sjostrand, S. Mrenna and P. Skands, *J. High Energy Phys.* **0605** (2006) 026.
 32. G. Corcella *et al.*, *J. High Energy Phys.* **0101** (2001) 010.
 33. T. Geisberg *et al.*, arXiv:0811.4622 (2008).
 34. F. Maltoni and T. Stelzer, *J. High Energy Phys.* **0302** (2003) 027; J. Alwall *et al.*, *J. High Energy Phys.* **0709** (2007) 028.
 35. A. Pukhov *et al.*, hep-ph/9908288.
 36. W. Kilian, T. Ohl and J. Reuter, arXiv:0708.4233.
 37. J. Alwall *et al.*, *Comput. Phys. Commun.* **176** (2007) 300.
 38. H. Baer, X. Tata and J. Woodside, Ref.¹⁸
 39. P. Mercadante, J. K. Mizukoshi and X. Tata, *Phys. Rev. D* **72** (2005) 035009; S. P. Das *et al.*, *Eur. Phys. J. C* **54** (2008) 645; R. Kadala, P. Mercadante, J. K. Mizukoshi and X. Tata, *Eur. Phys. J. C* **56** (2008) 511.
 40. H. Baer, A. Belyaev, T. Krupovnickas and X. Tata, *J. High Energy Phys.* **0402** (2004) 007; H. Baer, T. Krupovnickas and X. Tata, *J. High Energy Phys.* **0406** (2004) 061.
 41. H. Baer, H. Prosper and H. Summy, *Phys. Rev. D* **77** (2008) 055017.
 42. H. Baer, A. Lessa and H. Summy, arXiv:0809.4719 (2008).
 43. I. Hinchliffe *et al.*, *Phys. Rev. D* **55** (1997) 5520 and *Phys. Rev. D* **60** (1999) 095002.
 44. H. Baer, K. Hagiwara and X. Tata, *Phys. Rev. D* **35** (1987) 1598; H. Baer, D. Dzialo-Karatas and X. Tata, *Phys. Rev. D* **42** (1990) 2259; H. Baer, C.

- Kao and X. Tata, *Phys. Rev. D* **48** (1993) 5175; H. Baer, C. H. Chen, F. Paige and X. Tata, *Phys. Rev. D* **50** (1994) 4508.
45. R. Arnowitt *et al.* *Phys. Lett. B* **639** (2006) 46 and *Phys. Lett. B* **649** (2007) 73.
 46. H. Bachacou, I. Hinchliffe and F. Paige, *Phys. Rev. D* **62** (2000) 015009; Atlas Collaboration, LHCC 99-14/15.
 47. C. Lester and D Summers, *Phys. Lett. B* **463** (1999) 99; A. Barr, C. Lester and P. Stephens, *J. Phys. bf G29* (2003) 2343; C. Lester and A. Barr, *J. High Energy Phys.* **0712** (2007) 102; W. Cho, K. Choi, Y. Kim and C. Park, *J. High Energy Phys.* **0802** (2008) 035.
 48. H. Baer, V. Barger, G. Shaughnessy and H. Summy, *Phys. Rev. D* **75** (2007) 095010.
 49. K. Kawagoe *et al.* *Phys. Rev. D* **69** (2004) 035003; S. Ambrosanio *et al.* *J. High Energy Phys.* **0101** (2001) 014.
 50. H. Hamaguchi, S. Shirai and T. Yanagida, arXiv:0712.2462.
 51. J. Feng *et al.* *Phys. Rev. D* **52** (1995) 1418; M. Nojiri, K. Fujii and T. Tsukamoto, *Phys. Rev. D* **54** (1996) 6756.
 52. E. Baltz, M. Battaglia, M. Peskin and T. Wizansky, *Phys. Rev. D* **74** (2006) 103521. See also R. Arnowitt *et al.*, *Phys. Rev. Lett.* **100** (2008) 231802 for a similar study in the stau co-annihilation region.
 53. For a review, see D. Hooper and S. Profumo, *Phys. Rept.* **453** (2007) 29.
 54. H. C. Cheng, K. Matchev and M. Schmaltz, *Phys. Rev. D* **66** (2002) 036005.
 55. T. Rizzo, *Phys. Rev. D* **64** (2001) 095010; C. Macesanu, C. McMullen and S. Nandi, *Phys. Rev. D* **66** (2002) 015009.
 56. G. Servant and T. Tait, *Nucl. Phys. B* **650** (2003) 391; K. Kong and K. Matchev, *J. High Energy Phys.* **0601** (2006) 038.
 57. H. C. Cheng, K. Matchev and M. Schmaltz, *Phys. Rev. D* **66** (2002) 056006; A. Datta, K. Kong and K. Matchev, *Phys. Rev. D* **72** (2005) 096006.
 58. A. Alves, O. Eboli and T. Plehn, *Phys. Rev. D* **74** (2006) 095010.
 59. A. Birkedal, A. Noble, M. Perelstein and A. Spray, *Phys. Rev. D* **74** (2006) 035002; D. Hooper and G. Zaharijas, *Phys. Rev. D* **75** (2007) 035010.
 60. N. Arkani-Hamed, A. Cohen and H. Georgi, *Phys. Lett. B* **513** (2001) 232; N. Arkani-Hamed, A. Cohen, E. Katz and A. Nelson, *J. High Energy Phys.* **07** (2002) 034.
 61. For reviews, see M. Schmaltz, *Ann. Rev. Nucl. Part. Sci.* **55** (2005) 229 and M. Perelstein, *Prog. Part. Nucl. Phys.* **58** (2007) 247.
 62. H. C. Cheng and I. Low, *J. High Energy Phys.* **0309** (2003) 051.
 63. J. Hubisz and P. Meade, *Phys. Rev. D* **71** (2005) 035016.
 64. C. Hill and R. Hill *Phys. Rev. D* **75** (2007) 115009.
 65. H.-C. Cheng, arXiv:0710.3407 [hep-ph].
 66. C.-S. Chen, K. Cheung and T. C. Yuan, *Phys. Lett. B* **664** (2007) 158; T. Han, H. Logan and L.-T. Wang, *J. High Energy Phys.* **0601** (2006) 099.
 67. H. C. Cheng, I. Low and L. T. Wang, *Phys. Rev. D* **74** (2006) 055001; S. Matsumoto, M. Nojiri and D. Nomura, *Phys. Rev. D* **75** (2007) 055006; A. Belyaev, C. Chen, K. Tobe and C. P. Yuan, *Phys. Rev. D* **74** (2006) 115020; M. Carena, J. Hubisz, M. Perelstein and P. Verdier, *Phys. Rev. D* **75** (2007)

- 091701.
68. T. Han, R. Mahbubani, D. Walker and L. T. Wang, axViv:0803.3820 (2008).
69. Z. Chacko, H-S. Goh and R. Harnik, *Phys. Rev. Lett.* **96** (2006) 231802; see E. Dolle and S. Su, *Phys. Rev.* **D 77** (2008) 075013 for an analysis of DM in a twin-Higgs scenario.
70. Y. Bai, *Phys. Lett.* **B 666** (2008) 332.
71. P. Gondolo, J. Edsjo, P. Ullio, L. Bergstrom, M. Schelke and E. A. Baltz, *JCAP* **0407** (2004) 008.
72. G. Belanger, F. Boudjema, A. Pukhov and A. Semenov, *Comput. Phys. Commun.* **174** (2006) 577; *Comput. Phys. Commun.* **176** (2007) 367.
73. IsaRED, by H. Baer, C. Balazs and A. Belyaev, *J. High Energy Phys.* **0203** (2002) 042.
74. H. Baer and M. Brhlik, *Phys. Rev.* **D 53** (1996) 597; V. Barger and C. Kao, *Phys. Rev.* **D 57** (1998) 3131.
75. J. Ellis, T. Falk and K. Olive, *Phys. Lett.* **B 444** (1998) 367; J. Ellis, T. Falk, K. Olive and M. Srednicki, *Astropart. Phys.* **13** (2000) 181; M.E. Gómez, G. Lazarides and C. Pallis, *Phys. Rev.* **D 61** (2000) 123512 and *Phys. Lett.* **B 487** (2000) 313; A. Lahanas, D. V. Nanopoulos and V. Spanos, *Phys. Rev.* **D 62** (2000) 023515; R. Arnowitt, B. Dutta and Y. Santoso, *Nucl. Phys.* **B 606** (2001) 59; see also Ref.⁷³
76. K. L. Chan, U. Chattopadhyay and P. Nath, *Phys. Rev.* **D 58** (1998) 096004; J. Feng, K. Matchev and T. Moroi, *Phys. Rev. Lett.* **84** (2000) 2322 and *Phys. Rev.* **D 61** (2000) 075005; see also H. Baer, C. H. Chen, F. Paige and X. Tata, *Phys. Rev.* **D 52** (1995) 2746 and *Phys. Rev.* **D 53** (1996) 6241; H. Baer, C. H. Chen, M. Drees, F. Paige and X. Tata, *Phys. Rev.* **D 59** (1999) 055014; for a model-independent approach, see H. Baer, T. Krupovnickas, S. Profumo and P. Ullio, *J. High Energy Phys.* **0510** (2005) 020.
77. M. Drees and M. Nojiri, *Phys. Rev.* **D 47** (1993) 376; H. Baer and M. Brhlik, *Phys. Rev.* **D 57** (1998) 567; H. Baer, M. Brhlik, M. Diaz, J. Ferrandis, P. Mercadante, P. Quintana and X. Tata, *Phys. Rev.* **D 63** (2001) 015007; J. Ellis, T. Falk, G. Ganis, K. Olive and M. Srednicki, *Phys. Lett.* **B 510** (2001) 236; L. Roszkowski, R. Ruiz de Austri and T. Nihei, *J. High Energy Phys.* **0108** (2001) 024; A. Djouadi, M. Drees and J. L. Kneur, *J. High Energy Phys.* **0108** (2001) 055; A. Lahanas and V. Spanos, *Eur. Phys. J.* **C 23** (2002) 185.
78. R. Arnowitt and P. Nath, *Phys. Rev. Lett.* **70** (1993) 3696; H. Baer and M. Brhlik, Ref.⁷⁴; A. Djouadi, M. Drees and J. Kneur, *Phys. Lett.* **B 624** (2005) 60.
79. C. Böhm, A. Djouadi and M. Drees, *Phys. Rev.* **D 30** (2000) 035012; J. R. Ellis, K. A. Olive and Y. Santoso, *Astropart. Phys.* **18** (2003) 395; J. Edsjö, *et al.*, *JCAP* **0304** (2003) 001.
80. H. Baer, A. Mustafayev, E. Park and X. Tata, *J. High Energy Phys.* **0805** (2008) 058.
81. Z. Ahmed *et al.*, arXiv:0802:3530 [astro-ph].
82. J. Angle *et al.*, *Phys. Rev. Lett.* **100** (2008) 021303.
83. E. Behnk *et al.*, arXiv:0804:2886 [astro-ph]
84. H. Baer, A. Mustafayev, E. Park and X. Tata, *JCAP* **0701**, 017 (2007).

85. D. Feldman, Z. Liu and P. Nath, *Phys. Lett.* **B 662** (2008) 190.
86. R. Schnee, (CDMS Collaboration); A. M. Green, *JCAP* **0708** (2007) 022; C-L. Shan and M. Drees and C. L. Shan, *JCAP***0806** (2008) 012.
87. H. Baer, A. Belyaev, T. Krupovnickas and J. O’Farrill, *JCAP* **0408** (2004) 005.
88. H. Baer and J. O’Farrill, *JCAP***0404**, 005 (2004); H. Baer, C. Balazs, A. Belyaev and J. O’Farrill, *JCAP* **0309**, (2003) 007.
89. P. Sreekumar *et al.* [EGRET Collaboration], *Astrophys. J.* **494**, 523 (1998) [arXiv:astro-ph/9709257].
90. W. de Boer, M. Herold, C. Sander, V. Zhukov, A. V. Gladyshev and D. I. Kazakov, arXiv:astro-ph/0408272.
91. F. W. Stecker, S. D. Hunter and D. A. Kniffen, *Astropart. Phys.* **29** (2008) 25.
92. H. Baer, A. Belyaev and H. Summy, *Phys. Rev.* **D 77** (2008) 095013.
93. S. Weinberg, *Phys. Rev. Lett.* **48** (1982) 1303; R. H. Cyburt, J. Ellis, B. D. Fields and K. A. Olive, *Phys. Rev.* **D 67** (2003) 103521; K. Jedamzik, *Phys. Rev.* **D 70** (2004) 063524; M. Kawasaki, K. Kohri and T. Moroi, *Phys. Lett.* **B 625** (2005) 7 and *Phys. Rev.* **D 71** (2005) 083502; K. Kohri, T. Moroi and A. Yotsuyanagi, *Phys. Rev.* **D 73** (2006) 123511; M. Kawasaki, K. Kohri, T. Moroi and A. Yotsuyanagi, arXiv:0804.3745 (2008).
94. H. Pagels and J. Primack, *Phys. Rev. Lett.* **48** (1982) 223; J. Feng, A. Rajaraman and F. Takayama, *Phys. Rev. Lett.* **91** (2003) 011302 and *Phys. Rev.* **D 68** (2003) 085018.
95. M. Bolz, A. Brandenburg and W. Buchmuller, *Nucl. Phys.* **B 606** (2001) 518; J. Pradler and F. Steffen, *Phys. Rev.* **D 75** (2007) 023509.
96. K. Jedamzik, M. LeMoine and G. Moultaqa, *JCAP***0607** (2006) 010.
97. J. Feng, S. Su and F. Takayama, *Phys. Rev.* **D 70** (2004) 075019.
98. W. Buchmuller, P. Di Bari and M. Plumacher, *Annal. Phys.* **315** (2005) 305.
99. W. Buchmuller, L. Covi, J. Kersten, K. Schmidt-Hoberg, *JCAP***0611** (2006) 007; W. Buchmuller, L. Covi, K. Hamaguchi, A. Ibarra and T. Yanagida, *J. High Energy Phys.* **0703** (2007) 037.
100. R. Peccei and H. Quinn, *Phys. Rev. Lett.* **38** (1977) 1440 and *Phys. Rev.* **D 16** (1977) 1791; S. Weinberg, *Phys. Rev. Lett.* **40** (1978) 223; F. Wilczek, *Phys. Rev. Lett.* **40** (1978) 279.
101. J. E. Kim and H. P. Nilles, *Phys. Lett.* **B 138** (1984) 150.
102. L. Covi, J. E. Kim and L. Roszkowski, *Phys. Rev. Lett.* **82** (1999) 4180; L. Covi, H. B. Kim, J. E. Kim and L. Roszkowski, *J. High Energy Phys.* **0105** (2001) 033; L. Covi, L. Roszkowski and M. Small, *J. High Energy Phys.* **0207** (2002) 023.
103. A. Brandenburg and F. Steffen, *JCAP***0408** (2004) 008.
104. G. Lazarides and Q. Shafi, *Phys. Lett.* **B 258** (1991) 305; K. Kumekawa, T. Moroi and T. Yanagida, *Prog. Theor. Phys.* **92** (1994) 437; T. Asaka, K. Hamaguchi, M. Kawasaki and T. Yanagida, *Phys. Lett.* **B 464** (1999) 12.
105. H. Baer and J. Ferrandis, *Phys. Rev. Lett.* **87** (2001) 211803; D. Auto, H. Baer, C. Balazs, A. Belyaev, J. Ferrandis and X. Tata, *J. High Energy Phys.* **0306** (2003) 023; D. Auto, H. Baer and A. Belyaev and T. Krupovnickas, *J.*

- High Energy Phys.* **0410** (2004) 066; H. Baer, S. Kraml, S. Sekmen and H. Summy, *JHEP***0803**, 056 (2008).
106. T. Blazek, R. Dermisek and S. Raby, *Phys. Rev. Lett.* **88** (2002) 111804 and *Phys. Rev.* **D 65** (2002) 115004.
107. H. Baer, S. Kraml, S. Sekmen and H. Summy, *J. High Energy Phys.* **0810** (2008) 079.
108. H. Baer and H. Summy, *Phys. Lett.* **B 666** (2008) 5;
109. H. Baer, M. Haider, S. Kraml, S. Sekmen and H. Summy, arXiv:0812.2693 (2008).